INTERNATIONAL ATOMIC ENERGY AGENCY
UNITED NATIONS EDUCATIONAL, SCIENTIFIC AND CULTURAL ORGANIZATION

INTERNATIONAL CENTRE FOR THEORETICAL PHYSICS
34100 TRIESTE (ITALY) - P.O.B. 586 - MIRAMARE - STRADA COSTIERA 11 - TELEPHONES: 224281/2/3/4/5/6
CABLE: CENTRATOM - TELEX 460392-I

INTERNATIONAL CENTRE FOR THEORETICAL PHYSICS
21 MAR 1985
LIBRARY

SMR/115 - 35

WINTER COLLEGE ON LASERS, ATOMIC AND MOLECULAR PHYSICS

(21 January - 22 March 1985)

SEMICONDUCTOR LASERS & PICOSECOND OPTOELECTRONICS

Part II: Optical Properties

Part III: Picosecond Optoelectronics

E.O. GOEBEL
Max-Planck-Institut fuer Festkoerperforschung
Heisenbergstrasse, 1
Postfach 80 06 65
7000 Stuttgart 80
Fed. Rep. Germany

These are preliminary lecture notes, intended only for distribution to participants.
Missing or extra copies are available from Room 229.

PART II

OPTICAL PROPERTIES

- longitudinal mode spectrum
- coherence

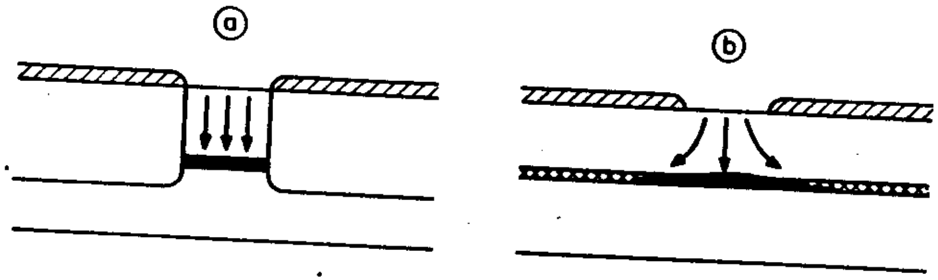

index guiding

$n(x) = n_r(x)$

gain guiding

$n(x) = n_r(x) + i\, n_i(x)$

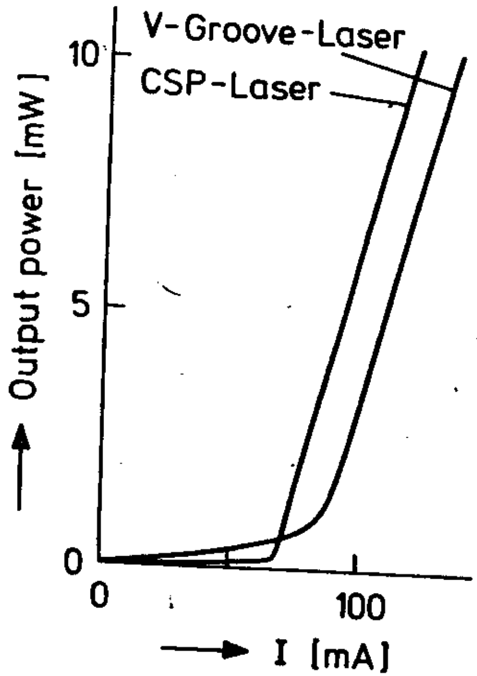

gain-guided

index-guided

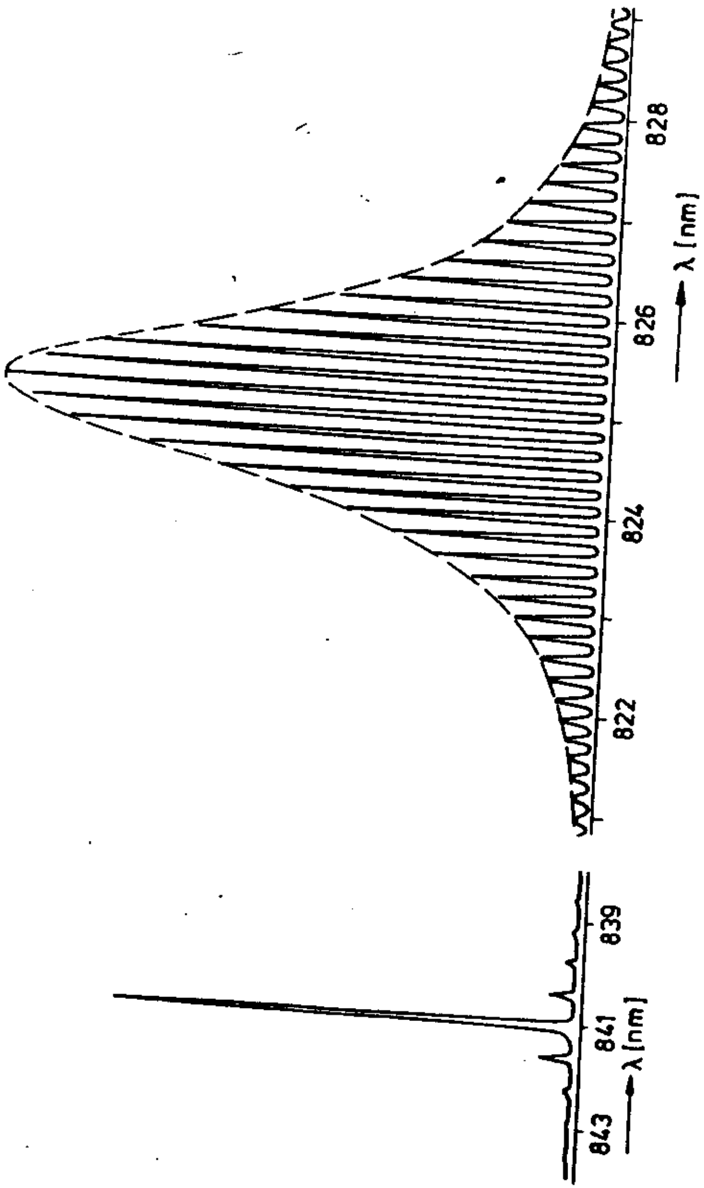

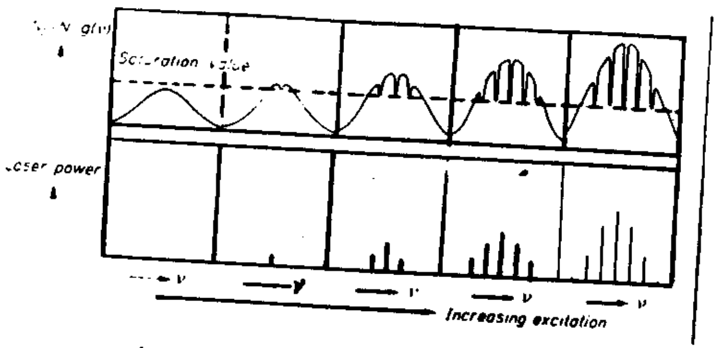

Inhomogeneous Broadening
(spectral hole burning)

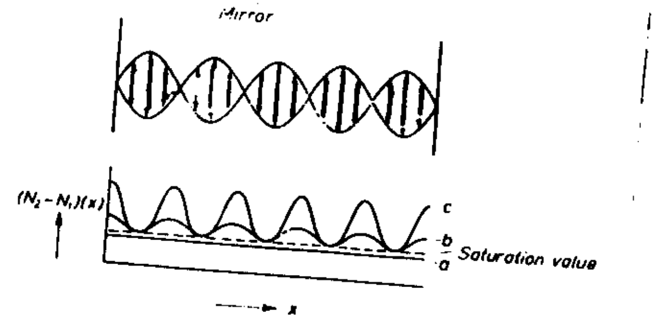

Spatial hole burning

spectral hole burning?

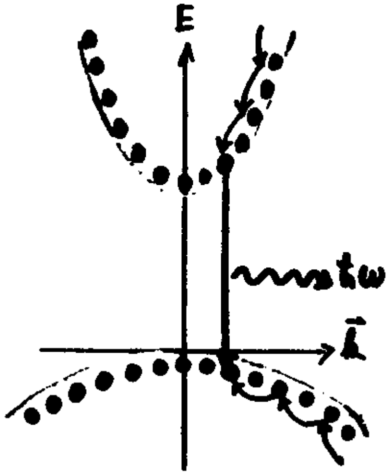

$\tau_{e,e}, \tau_{h,h} < 10^{-12}\,s$
(W. Graudszus, Stuttgart)

no!

(see also: W. Rühle et al.
IEEE Journ. Quant. Electr.
QE-17, 714 (1981))

spatial hole burning?

$L_D \sim 1\mu m \ldots 10\mu m$

distance of the "holes": $d = \frac{\lambda_{vac}}{2 \cdot n}$

$\simeq 0.25\mu m \; (\lambda = 0.9\mu m)$
$\simeq 0.37\mu m \; (\lambda = 1.3\mu m)$

no!

semiconductor laser should be single mode!

Multimode ↔ spontaneous emission

rate equations:

$$\frac{dN_e}{dt} = \frac{J}{e \cdot d} - A \sum_i g_i N_{ph,i} - \frac{N_e}{\tau_{spon}}$$

$$\frac{dN_{ph,i}}{dt} = A g_i N_{ph,i} - \frac{N_{ph,i}}{\tau_{stim}} + \alpha \frac{N_e}{\tau_{spon}}$$

$$\alpha = \frac{\text{spontaneous emission into mode } i}{\text{total spontaneous emission}}$$

α large: amplified spontaneous emission
α small: laser

$$\boxed{\alpha = \alpha_0 (V_{eff}) \cdot K}$$

K = astigmatism factor

K = 1 for index guided lasers
$K \simeq 10 \ldots 90$ for gain guided (GaAs) lasers
$\alpha_0 \simeq 10^{-5}$

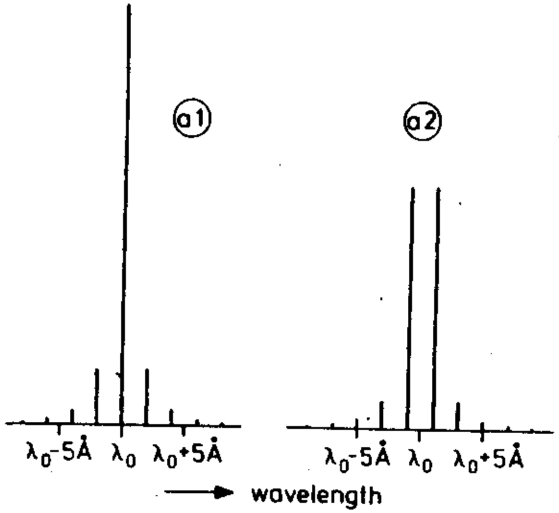

$d = 10^{-5}$

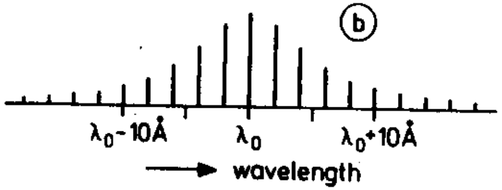

$d = 10^{-4}$

K. Petermann, Opt. and Quant. Electr. 12, 207 (1980)

Astigmatism:

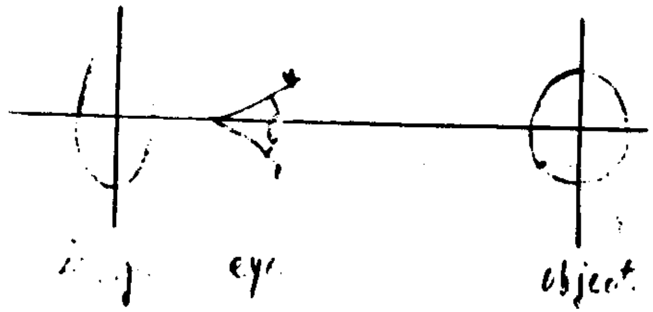

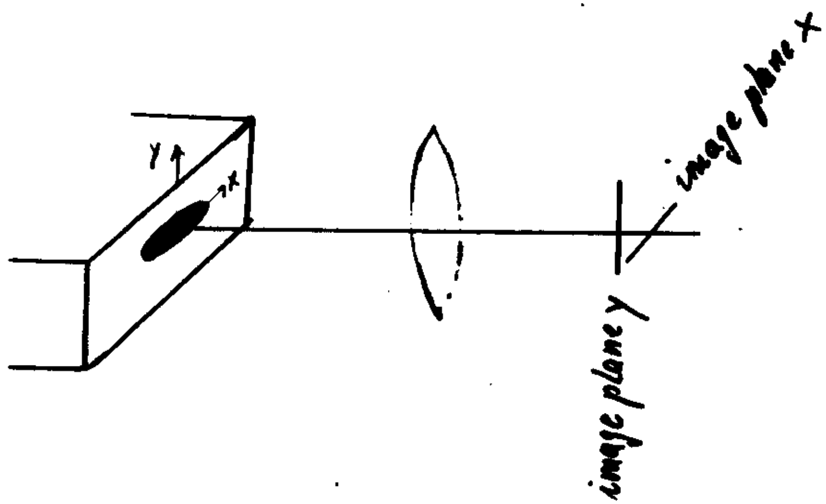

affects:

- near field measurements (be careful)
- far fields (ears)
- spont. emission factor
- coupling into fibres

origin of the astigmatism:

- curved phase fronts (in one dimension)

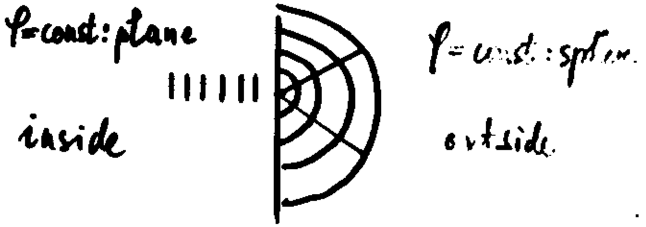

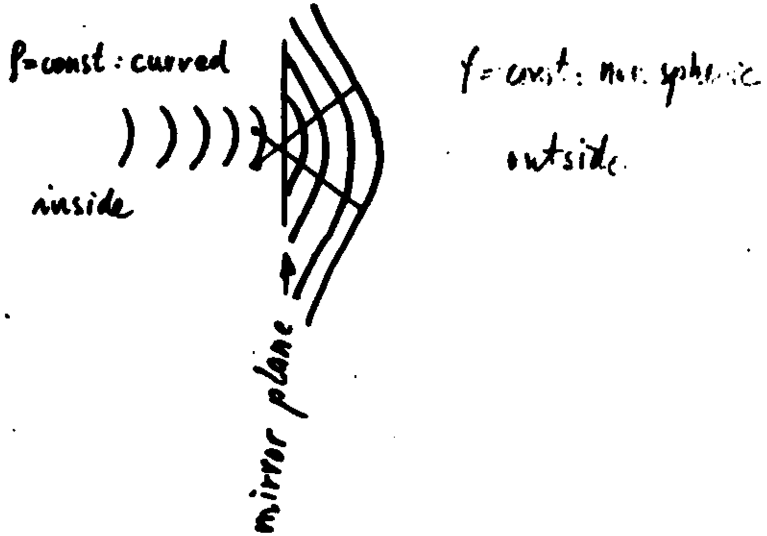

Calculation of φ = const

solve waveequation for:

$$\varepsilon = \varepsilon(x) = \varepsilon_0 - \varepsilon'(x)$$

$$\varepsilon'(x) = \varepsilon'_r(x) + i\,\varepsilon'_i(x)$$

$$\varepsilon_0 = \varepsilon_{0r} + i\,\varepsilon_{0i}$$

for example: $\varepsilon'(x) = a^2 x^2 \quad (a = a_r + i a_i)$

$\Rightarrow$

$$E(x,z) = e^{(-i\beta_r z)} \cdot e^{(\beta_i z)} \cdot e^{(-\frac{1}{2} i k a_i x^2)} \cdot e^{(-\frac{1}{2} k a_r x^2)}$$

phase factors

if $a_i = 0$: plane wavefronts

$\Rightarrow$ index guided lasers don't have an astigmatism

$a_i \neq 0$:

$\Psi = \text{const}: \ \beta_r z + \frac{1}{2} k a_i x^2 = \text{const}$

cylindrical wave front

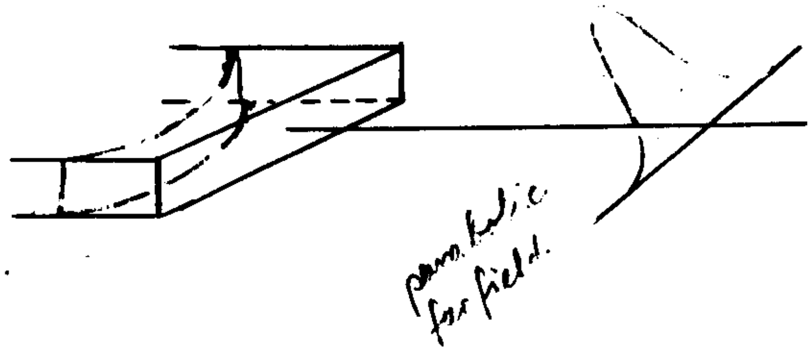

$\varepsilon'(x) = \cosh^{-2}(ax)$:

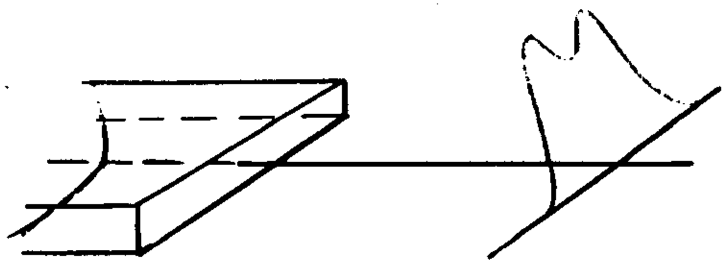

Astigmatism ↔ spont. emission factor

normally: $R_{spon} / R_{stim} = \frac{1}{N}$ (Einstein rel.)

(N = number of photons within one mode)

this is true only, if the modes are orthonormal (orthogonal and complete)

this is true only, if Hamiltonian is "hermitian"

curved wavefronts ≡ non hermitian H

$$\Psi_{gain\ guided} = \sum_{n=1}^{M} c_n \phi_n$$

↙ complete (Einstein rel. is not valid.) ⇓ number of spont. photons per lasing mode = M·1

↘ complete & orthogonal (Einstein rel. is valid.) ⇓ number of spont. photons per lasing mode ≡ 1

E. G...: Optical Communication (Springer

Yariv & Margalit, Journ. Quant. Elect. QE 18, 1831 (82)

K. T...kermann, ibid. QE-15, 566 (1979)

D. Marcuse, Electr. Lett. 18, 920 (1982)

W. Elsässer, E. Göbel, Electr. Lett. 19, 335 (1983)

EINSTEIN RELATIONS FOR GAIN-GUIDED SEMICONDUCTOR LASERS

Indexing terms: Lasers and laser applications, Semiconductor lasers, Quantum theory

The Einstein equations which relate the transition rates for stimulated emission, spontaneous emission and stimulated absorption in a laser active medium are re-examined for the special case of a semiconductor laser with complex waveguiding. It is shown that, owing to the nonorthogonality of the gain-guided laser modes, the Einstein relations have to be modified. In particular, the spontaneous emission rate per laser mode no longer equals the stimulated emission rate per laser photon.

Introduction: Gain-guided lasers differ in many aspects from index-guided lasers. The major reason for this is the enhancement of the spontaneous emission rate per laser mode due to the astigmatism.[1-3] Recently, Yariv[4] and Marcuse[5] have given a quantum mechanical explanation for this astigmatism induced increase of the spontaneous emission. According to these authors, the longitudinal gain-guided modes are not energy-orthogonal, and thus each of the gain-guided longitudinal modes has to be represented by a set of orthogonal mode functions. For these orthogonal mode functions the 'usual' Einstein relations[6] are valid.

In this letter we will show that this nonorthogonality of the longitudinal gain-guided laser modes requires a modification of the Einstein relation such that the spontaneous emission rate per laser mode is equal to the stimulated emission rate per laser photon multiplied by the astigmatism factor K (sometimes also referred to as the spontaneous emission enhancement factor). The 'usual' Einstein relation[6] is included as it is valid for index-guided lasers because the astigmatism factor is equal to one for these lasers.

Calculation of the Einstein relations: Following the analysis given in References 4 and 5, each gain-guided mode can be represented by M orthogonal modes ϕ_n, i.e. ϕ is the mode subspace which spans ψ:[5]

$$\psi = \sum_{n=1}^{M} c_n \phi_n \qquad (1)$$

For each of the modes ϕ_n the usual laser equations are valid, and in particular the absorption, stimulated and spontaneous emission rates per volume and energy interval can be written as:[7]

$$r_{abs} = n_p(\hbar\omega) \int_0^\infty M(\hbar\omega, \varepsilon) n_o(\varepsilon) n_u(\varepsilon + \hbar\omega)\, d\varepsilon$$

$$r_{stim} = n_p(\hbar\omega) \int_0^\infty M(\hbar\omega, \varepsilon) n_u(\varepsilon) n_o(\varepsilon + \hbar\omega)\, d\varepsilon \qquad (2)$$

$$r_{spon} = D_p(\hbar\omega) \int_0^\infty M(\hbar\omega, \varepsilon) n_u(\varepsilon) n_o(\varepsilon + \hbar\omega)\, d\varepsilon$$

where n_o and n_u denote the occupied and unoccupied band states, respectively, $M(\hbar\omega, \varepsilon)$ contains the matrix element for the transition, $n_p(\hbar\omega)$ is the photon density and $D_p(\hbar\omega) = [n^3(\hbar\omega)^2]/(\pi^2\hbar^3c^3)$, the density of states for photons in a cavity with refractive index n. In particular, eqns. 2 are valid for the energy interval $\Delta\phi_n$ which defines a single mode ϕ_n. The balance conditions for upward and downward transitions per mode interval $\Delta\phi_n$ can thus be written as

$$\frac{r_{spon}}{\Delta\phi_n} + \frac{r_{stim}}{\Delta\phi_n} - \frac{r_{abs}}{\Delta\phi_n} = 0 \qquad (3)$$

Inserting the Fermi distribution functions[7] for n_o and n_u in eqns. 2, eqn. 3 results in

$$\frac{r_{spon}}{\Delta\phi_n} = \frac{r_{stim}}{\Delta\phi_n} \left\{ \exp\left[\frac{\hbar\omega - (\mu_c - \mu_v)}{kT} \right] - 1 \right\} \qquad (4)$$

with $\mu_c - \mu_v$ as the difference in the chemical potentials of conduction and valence band.

$$f_p(\hbar\omega) = \left\{ \exp\left[\frac{\hbar\omega - (\mu_c - \mu_v)}{kT} \right] - 1 \right\}^{-1} \qquad (5)$$

is the generalised photon distribution function (not only for thermal black-body radiation),[7] i.e. $f_p(\hbar\omega)$ is equal to the number of photons n per laser mode interval $\Delta\phi_n$, and hence eqn. 4 can be rewritten as

$$\frac{r_{spon}}{\Delta\phi_n} = \frac{r_{stim}}{\Delta\phi_n} \frac{1}{\frac{n}{\Delta\phi_n}} = \frac{r_{stim}}{n} \qquad (6)$$

Eqn. 6 is usually referred to as the Einstein relation.[6] Since M mode intervals $\Delta\phi_n$ are required to build up the energy interval $\Delta\psi$ of one real laser mode ψ, we have M equations. The spontaneous emission rate per gain-guided longitudinal laser mode $R_{spon}/\Delta\psi$ is obtained by summing up these M equations:

$$\frac{R_{spon}}{\Delta\psi} = \sum_{n=1}^{M} \frac{r_{spon}}{\Delta\phi_n} = M \frac{r_{spon}}{\Delta\phi_n} = M \frac{r_{stim}}{n} \qquad (7)$$

For simplicity, it has been assumed that r_{spon} and r_{stim} are the same for all the M modes ϕ_n.

The number of submodes M which is needed to represent one gain-guided mode ψ is equal to the spontaneous emission factor K,[5] and thus it follows from eqn. 7 that the spontaneous emission rate per gain-guided laser mode, $R_{spon/mode} = R_{spon}/\Delta\psi$, is connected with the stimulated emission rate per photon, $r_{stim/phot} = r_{stim}/n$, as follows:

$$R_{spon/mode} = K r_{stim/phot} \qquad (8)$$

In contrast to the 'usual' Einstein relation, where the spontaneous emission rate per mode is equal to the stimulated emission rate per photon, we now obtain for gain-guided lasers that the spontaneous emission rate per laser mode $R_{spon/mode}$ is equal to the stimulated emission rate per laser photon $r_{stim/phot}$ multiplied by the astigmatism factor K.

The stimulated emission rate per photon is connected with other laser parameters via

$$r_{stim/phot} = v_g g n_{sp} \qquad (9)$$

where v_g denotes the group velocity, g the optical gain and n_{sp} accounts for incomplete population inversion, and hence

$$R_{spon/mode} = K v_g g n_{sp} \qquad (10)$$

Eqns. 8 and 10 thus represent the modified Einstein equations for gain-guided lasers. It is important to realise that the spontaneous emission rate per laser mode enters directly into the spectral linewidth of the individual laser modes. On the basis of the analysis presented above we can therefore prove that the observed difference in power dependence of the laser linewidth for gain- and index-guided laser[8] results from the difference in the astigmatism factor.

Summary: We have re-examined the balance equations for emission and absorption processes in gain-guided lasers. It has been shown that the nonorthogonality of the gain-guided longitudinal laser modes results in a modified Einstein relation. According to this Einstein relation, the spontaneous emission rate per laser mode is obtained by multiplication of the stimulated emission rate per laser photon with the astigmatism factor K.

Acknowledgment: Support from the Deutsche Forschungsgemeinschaft is gratefully acknowledged.

W. ELSÄSSER
E. O. GÖBEL

Max-Planck-Institut für Festkörperforschung
Heisenbergstrasse 1
7000 Stuttgart 80, W. Germany

22nd March 1983

References

1 PETERMANN, K.: 'Calculated spontaneous emission factor for double-heterostructure injection lasers with gain-induced waveguiding', *IEEE J. Quantum Electron.*, 1979, QE-15, pp. 566–570
2 STREIFER, W., SCIFRES, D. R., and BURNHAM, R. D.: 'Spontaneous emission factor of narrow-stripe gain-guided diode lasers', *Electron. Lett.*, 1981, 17, pp. 933–934
3 WITTKE, J. P.: 'Spontaneous-emission-rate alteration by dielectric and other waveguiding structures', *RCA Rev.*, 1975, 36, pp. 655–666
4 YARIV, A., and MARGALIT, S.: 'On spontaneous emission into guided modes with curved wavefronts', *IEEE J. Quantum Electron.*, 1982, QE-18, pp. 1831–1832
5 MARCUSE, D.: 'Quantum mechanical explanation of the spontaneous emission K-factor', *Electron. Lett.*, 1982, 18, pp. 920–922
6 HAKEN, H.: 'Encyclopedia of physics, Vol. XXV/2c', FLÜGGE, S. (Ed.), (Springer, Berlin, 1970), p. 92
7 WÜRFEL, P.: 'The chemical potential of radiation', *J. Phys. C*, 1982, 15, pp. 3967–3985
8 ELSÄSSER, W., GÖBEL, E. O., and KUHL, J.: 'Coherence properties of gain and index guided semiconductor lasers', *IEEE J. Quantum Electron.*, 1983, QE-19, to be published

0013-5194/83/090335-02$1.50/0

On Spontaneous Emission Into Guided Modes with Curved Wavefronts

AMNON YARIV AND SHLOMO MARGALIT

Abstract—The problem of spontaneous emission into guided modes with curved wavefronts is examined quantum mechanically. A classical result due to Petermann, which shows an increased emission rate relative to modes with planar phase fronts, is corroborated.

THE amount of power which is emitted spontaneously into a laser mode plays an important role in determining the spectral and dynamic features of the laser radiation. It figures prominently in semiconductor lasers in questions such as the resonance peak ("spiking resonance") in the modulation response as well as in the number of longitudinal modes which oscillate [2].

An important result due to Petermann [3] is that the spontaneous emission power into modes with curved wavefronts (such as result from gain guiding or a combination of gain and (anti) real-index guiding) is enhanced relative to that emitted into modes in pure index guiding.

At first glance, this result seems to contradict [4] the basic quantum mechanical relationship which states that the ratio of stimulated to spontaneous emission rates into a (any) mode is equal to the number of quanta in the mode. This last statement would suggest that, all other factors remaining the same, the spontaneous emission rates into curved wavefront modes and those with planar wavefronts are equal. This apparent contradiction is not resolved by a study of Petermann's paper [3], which treats the electron in a semiconductor as a localized classical dipole. This classical approach which, in our opinion, still needs to be justified, does not make any contact with the conventional quantum mechanical derivation of the spontaneous emission [5] rate.

To resolve this problem, we undertook a quantum mechanical derivation of the spontaneous emission problem into a mode with a field dependence

$$E(x,z) = E_o \exp\left[-\frac{x^2}{2\omega^2}(1+i\chi) - i\beta z\right] \tag{1}$$

corresponding to a Gaussian beam height ω [2] and a radius of curvature of the wavefront $R = 2\pi n\omega^2/\chi\lambda$. In a real-index-guided mode, the astigmatism factor χ is zero, while in the case of pure gain guiding, $\chi = 1$. Higher values of χ obtain in a combination of anti-index guiding and gain guiding [3]. The key idea is that when $\chi \neq 0$, the field (1) *does not qualify* as a quantum mechanical mode. A "proper" mode must be an eigenfunction of a field Hamiltonian $\hat{H}_{\text{field}}$ with the total $\hat{H}$ of the form

$$\hat{H} = \hat{H}_{\text{field}} + \hat{H}_{\text{electron}} + \hat{H}_{\text{interaction}}. \tag{2}$$

Manuscript received July 6, 1982. This work was supported by the Office of Naval Research and the Air Force Office of Scientific Research.

The authors are with the California Institute of Technology, Pasadena, CA 91125.

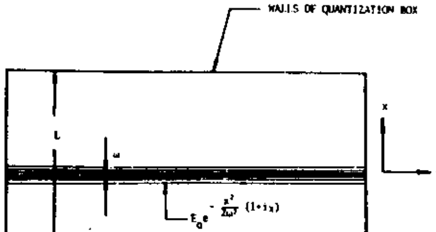

Fig. 1. Schematic representation of the gain guided mode inside an arbitrarily large (height L) quantization box.

The curved wavefront modes cannot exist without the electrons since they depend for their existence on the presence of of a transverse gain profile [5]. The total mode-electron system is, consequently, not described by a Hamiltonian such as (2). Since $\hat{H}_{\text{field}}$ does not exist independently of $\hat{H}_{\text{electron}}$, we will, consequently, refer to such modes as "improper modes." It follows that the standard quantum mechanical result concerning the ratio of stimulated to spontaneous transition rates *does not apply* to "improper modes."

To analyze the problem quantum mechanically, we "place" the laser structure inside an arbitrarily large (height L) quantization box as shown in Fig. 1.

The "big box" modes are of the form $e^{i[\omega t - k_z z + l(2\pi/L)x]}$ where $k_z^2 + (l(2\pi/L))^2 = (2\pi n/\lambda)^2$. The spontaneous emission rate into any one of these modes is given by the standard quantum mechanical result since these modes are defined (and exist) without injected electrons so that the total system Hamiltonian is given by (2).

The calculation of the spontaneous emission rate is thus reduced to that of determining how many "big box" modes are needed to expand the "improper mode" and then summing the spontaneous rates into these modes. The result is the spontaneous transition rate into the "improper mode." Let

$$\exp\left[-\frac{x^2}{2\omega^2}(1+i\chi)\right] = \sum_{-\infty}^{\infty} A_l \exp il\frac{2\pi}{L}x \tag{3}$$

from which

$$A_l = \frac{\omega}{L}\sqrt{\frac{2\pi}{1+i\chi}}\exp\left[-\frac{2l^2\pi^2\omega^2(1-i\chi)}{L^2(1+\chi^2)}\right]. \tag{4}$$

By approximating the effective number of modes $N \equiv 2l$ by the value of l where $|A_l| = e^{-1}|A_o|$, we obtain

$$N = \frac{\sqrt{2}}{\pi}\frac{L}{\omega}\sqrt{1+\chi^2}. \tag{5}$$

The total spontaneous emission rate into an improper mode is equal to the spontaneous rate into one "big box" mode multiplied by the number N of "big box" modes contained in the improper mode.

Since the spontaneous emission rate into a proper mode is inversely proportional to the mode volume, we have

$$(W_{\text{spont}}) \text{ into improper mode} \approx A\frac{L}{\omega}\sqrt{1+\chi^2}\ \frac{1}{L} \tag{6}$$

where A is some constant. The rate of spontaneous emission into a proper real-index guided mode with the same Gaussian beam radius ω as the improper mode is

$$(W_{\text{spont}}) \text{ into index guided mode} = A \times \left(\frac{1}{\omega}\right). \tag{7}$$

The factors $1/L$ and $1/\omega$ in the last two relations reflect the effective mode heights.

The ratio of the spontaneous emission rates into an "improper mode" and an index guided mode, both with the same beam radius ω, is thus

$$\frac{(W_{\text{spont}}) \text{ "improper"}}{(W_{\text{spont}}) \text{ index guided}} = \sqrt{1+\chi^2}. \tag{8}$$

This is the result obtained by Petermann using a classical dipole model for spontaneous transitions.

The rate of stimulated transition into the "improper" and index guided modes with the same ω is the same when both carry equal power. It follows immediately that the ratio of the rate of induced transition to that of spontaneous transition into an "improper mode" with a constant beam height ω and astigmatism factor χ is equal to the number of quanta in the mode divided by $\sqrt{1+\chi^2}$. The result is thus fully consistent with quantum mechanics.

References

[1] Y. Suematsu and K. Furuya, "Theoretical spontaneous emission factor of injection lasers," *Trans. IECE Japan*, vol. E.60, pp. 467–471, 1977.
[2] W. Streifer, D. R. Scifres, and R. D. Burnham, "Longitudinal mode spectra of diode lasers," *Appl. Phys. Lett.*, vol. 40, pp. 305–307, 1982.
[3] K. Petermann, "Calculated spontaneous emission factor for double heterostructure injection lasers with gain-induced wave-guiding," *IEEE J. Quantum Electron.*, vol. QE-15, pp. 566–570, July 1979.
[4] E. Patzak, "Spontaneous emission factor of narrow-stripe gain-guided diode lasers," *Electron. Lett.*, vol. 18, pp. 278–279, 1982.
[5] A. Yariv, *Quantum Electronics*, 2nd ed. New York: Wiley, 1975.

New Recombination Lasers in Li, Al, Ca, and Cu in a Segmented Plasma Device Employing Foil Electrodes

J. J. MACKLIN, OBERT R. WOOD, II, AND W. T. SILFVAST

Abstract—The use of foil electrodes in an expanding plasma recombination laser device has resulted in the generation of 30 laser transitions in Li I, Al I, Al II, Al III, Ca I, Ca II, Cu I, and Cu II. The generation of segmented arc plasmas in these metal vapors at the background gas pressures required for laser action had not previously been possible using bulk electrodes, and suggests that conditions necessary for recombination laser action may be obtained for any metal using this technique.

A LARGE number of metal-vapor recombination lasers with operating wavelengths from the UV to the mid-IR have recently been demonstrated using a segmented-plasma excitation-recombination (SPER) device [1]–[3]. Both the number and the type of metals studied thus far have been limited, however, by the undesirable occurrence, for some metals, of discharges in the He background gas which shorts out most (or all) of the sequential metal-vapor arcs and reduces (or eliminates) the laser gain. For example, a SPER device employing bulk electrodes (the type of electrodes used in previous SPER devices) of Li, Al, Ca, or Cu cannot be operated at He pressures below about 50 torr. On the other hand, a SPER device employing foil electrodes of these metals can easily be operated at low He pressures where laser action typically occurs (1–10 torr). This new foil electrode device has resulted in 30 new recombination laser transitions in these four metals at wavelengths ranging from 569.6 to 5460 nm. Twenty-eight of these transitions have not previously been observed in laser action. Except for a recent experiment involving the observation of a two-photon laser via optical pumping [4], this letter is the first report of laser action in lithium vapor. Isoelectronic scaling of the new laser transi-

Manuscript received July 9, 1982.

The authors are with Bell Laboratories, Holmdel, NJ 07733.

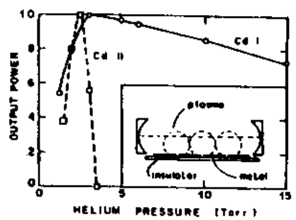

Fig. 1. Relative output power from a Cd SPER laser operating on the 1.433 μm transition in Cd I and the 537.8 nm transition in Cd II as a function of He pressure. Inset shows a highly schematic diagram of the experimental arrangement for a SPER device.

G. Grau - Spontaneous Emission into Index-Guided and Gain-Guided ...

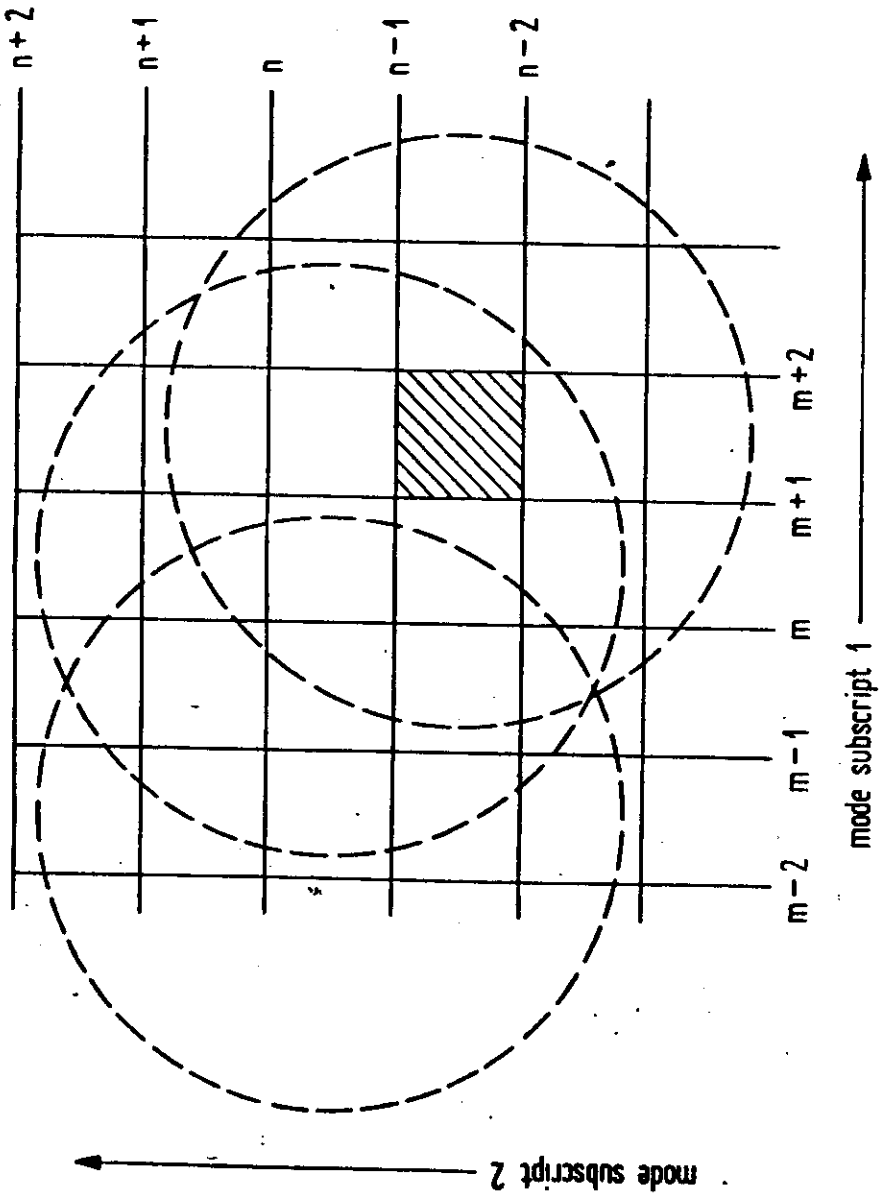

Coherence

$$L_{coh} = \frac{c}{\Delta\nu} .$$

$$\Delta\nu = \frac{h\nu \; v_g \; \alpha_m \; R_{spon}}{8\pi \cdot P_m} (1+\alpha)^2$$

enhancement term α (self coupling)

(modified Schawlow Townes formula)

C. Henry, IEEE J. Quant. Electr. QE-18, 259 (82)

$\Delta\nu = \beta(\text{MHz}\cdot\text{mW})P_m^{-1} + \Delta\nu_0$

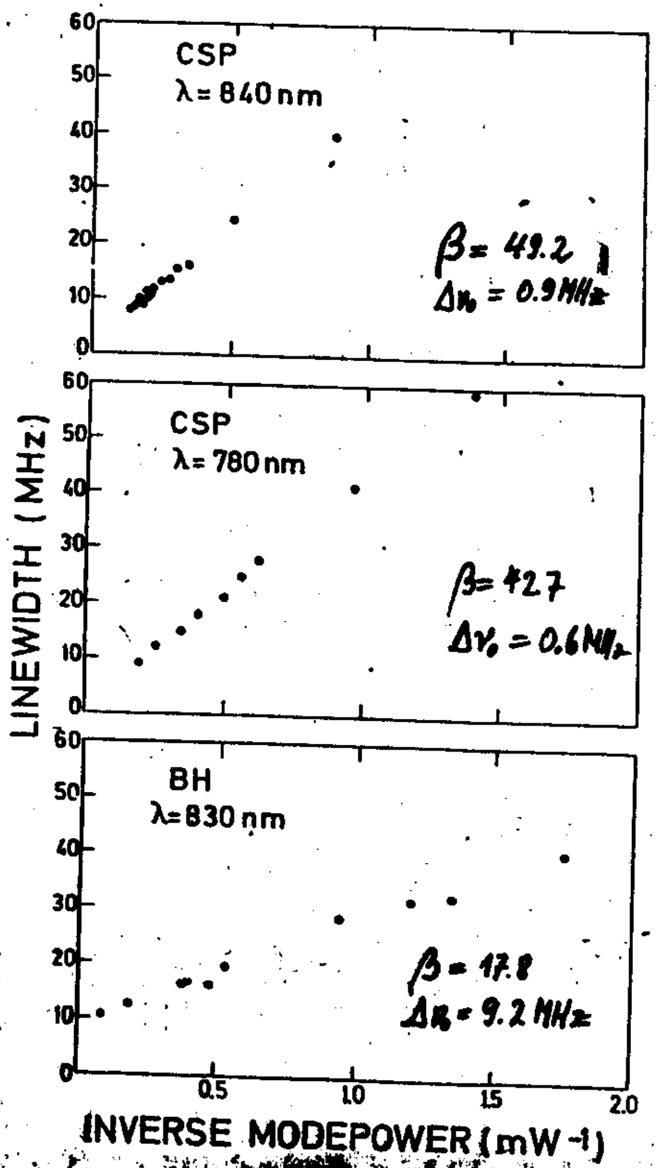

IEEE JOURNAL OF QUANTUM ELECTRONICS, VOL. QE-19, NO. 6, JUNE 1983 981

Coherence Properties of Gain- and Index-Guided Semiconductor Lasers

WOLFGANG ELSÄSSER, ERNST O. GÖBEL, AND JÜRGEN KUHL

Abstract—The spectral linewidth of the longitudinal laser modes has been measured as a function of mode power for different types of gain-guided as well as index-guided (GaAl)As double heterostructure laser diodes. Various effects contributing to line broadening, such as spontaneous emission, carrier density fluctuations, changes of the resonator parameters, and mode competition are discussed.

Introduction

HIGH temporal coherence is one of the characteristic features of laser light. In a "classical" laser, e.g., a gas or solid-state laser, the coherence properties are determined by the Q value of the cavity, the photon density within the cavity, and the spontaneous emission rate as described by the Schawlow-Townes formula [1]. Semiconductor lasers differ from gas or solid-state lasers with respect to the coherence properties essentially in the rate of spontaneous emission at each of the cavity mode frequencies. This spontaneous emission is several orders of magnitude higher in semiconductor lasers [2] resulting in reduced coherence. In addition, several line-broadening mechanisms which are not considered in the Schawlow-Townes formula have to be taken into account in semiconductor lasers, e.g., index fluctuations accompanying spontaneous events [3], [4] and fluctuations in the number of the electrons and holes [5].

Linewidth measurements for single longitudinal mode index-guided lasers have been reported recently [3], [5]-[7]. The linewidth is typically in the megahertz regime, corresponding to a coherence length of 10-100 m. Gain-guided lasers, which typically show a multimode emission spectrum, exhibit larger linewidths of the individual modes [8]. However, no comprehensive and detailed investigations on the mode power dependence of their linewidth have been published so far.

In this paper, we report detailed studies of the dependence of the laser linewidth on emitted light power per laser mode for various GaAs/(GaAl)As laser structures, namely, visible and infrared channeled substrate planar (CSP), infrared buried heterostructure (BH), V-groove, and oxide stripe lasers. For all the different index-guided lasers, we find a power-independent contribution to the linewidth, which is typically on the order of 1 MHz. This power-independent contribution can be partly attributed to density fluctuations, as discussed in [5]. The decrease of the laser linewidth with increasing mode power, furthermore, is stronger by a factor of 30 than expected from the Schawlow-Townes relation. This behavior has been explained by additional line broadening, due to index fluctuations initiated by the spontaneous emission [4].

The power-independent linewidth broadening of the gain-guided lasers is about three orders of magnitude larger than for the index-guided lasers. We attribute this large linewidth to phase fluctuations introduced by competition of the longitudinal laser modes. The decrease in linewidth with increasing mode power is even stronger in the gain-guided lasers than in the index-guided lasers, which is a consequence of the higher spontaneous emission rate per laser mode, due to the astigmatism.

Experimental

The following laser types have been investigated: CSP lasers (Hitachi) emitting in the infrared (840 nm) and visible (780 nm) spectral range; BH lasers (Hitachi); oxide stripe lasers (Siemens); and V-groove lasers (AEG-Telefunken), all emitting in the infrared. Typical data of the lasers, e.g., threshold current I_{th}, emission wavelength λ, mode spacing $\Delta\lambda_{mode}$, and emission characteristics are summarized in Table I. The lasers were mounted in a temperature-stabilized copper block to achieve a constant temperature of 298 K. The measurements were performed under CW conditions, except in the case of gain-guided lasers where the highest output powers (from 10-150 mW peak power) were achieved by pulsed operation (square pulses, 400 ns duration, repetition rate of 5 kHz). The emission spectrum was measured by a 1.0 m Czerny-Turner grating spectrometer equipped with a photomultiplier or an optical multichannel analyzer system. In the case of pulsed operation, a boxcar integrator with a gate width of 50 ns was used for signal averaging. The gate was set close to the end of the 400 ns excitation pulse to ensure quasi-stationary conditions.

Different instruments have been used for the linewidth determination, depending on the resolution required; a) a 1 m grating spectrometer (up to 10 GHz), b) a 1 m spectrometer with a plane Fabry-Perot interfermoter (up to 50 MHz), and c) a 1 m spectrometer with a 50 cm confocal Fabry-Perot interferometer (up to 1 MHz).

Great care has been taken in the case of index-guided lasers to avoid optical feedback by reflecting surfaces. This feedback showed up in a drastic linewidth narrowing and in an extreme sensitivity of the spectrum to mechanical distortion. The feedback was eliminated using antireflecting coatings for the optical components and by inserting neutral density filters between the laser and the spectrometer. The spectral output of the rear mirror of the semiconductor laser was simultaneously monitored to ensure that no feedback occurred.

The Fabry-Perot scans were recorded by a digital oscillo-

Manuscript received September 27, 1982; revised January 26, 1983. This work was supported by the Deutsche Forschungsgemeinschaft.

The authors are with the Max-Planck-Institut für Festkörperforschung, Stuttgart, West Germany.

0018-9197/83/0600-0981$01.00 © 1983 IEEE

TABLE I
TYPICAL DATA OF THE INVESTIGATED SEMICONDUCTOR LASERS AND RESULTS FOR THE INDIVIDUAL LASER MODE LINEWIDTH OBTAINED FROM LEAST-SQUARE FITS TO OUR EXPERIMENTAL DATA POINTS

laser type	BH	CSP	CSP	V-groove	oxide stripe
emission characteristic	single mode	single mode	single mode	multimode	multimode
guiding mechanism	index	index	index	gain	gain
λ (nm)	834	843	789	860	880
J_{th} (mA)	165	87	68	102	115
$\Delta\lambda_{mode}$ (Å)	2.83	2.80	2.57	1.97	2.30
$\Delta\nu_0$ (MHz)	9.2	0.9	0.6	6455	6409
$\partial\Delta\nu/\partial P^{-1}$ (MHz mW)	17.8	48.3	42.7	385	376

scope and transfered to a computer to evaluate the linewidth. The final result for the linewidth is obtained by averaging about 20 single scans.

The output power of the laser was measured with a calibrated silicon photodiode. Light power versus current showed a linear dependence in the entire investigated current range. The power per laser mode P_{mode} (per facet) in the case of multimode emission (gain-guided lasers) was determined from the emission spectrum and the total emitted power P_{tot} (per facet) according to

$$P_{mode} = P_{tot} \left\{ \int_{\lambda_i - \Delta\lambda/2}^{\lambda_i + \Delta\lambda/2} I(\lambda)\, d\lambda \Big/ \int_0^{\infty} I(\lambda)\, d\lambda \right\}$$

with intensity I, mode separation $\Delta\lambda$, and wavelength λ_i of the respective longitudinal laser mode.

Finally, near- and far-field patterns of the laser have been measured in the standard manner [9].

RESULTS

Experimental results for three different index-guided lasers are summarized in Fig. 1. We find a linear relation between linewidth and inverse optical mode power (per facet) P^{-1}_{mode} for all three lasers. A slope of 17.8 MHz · mW (infrared BH), 48.3 MHz · mW (infrared CSP), and 42.7 MHz · mW (visible CSP), and an intercept for $(P^{-1}_{mode}) = 0$ (e.g., infinite mode power) of 9.2 MHz (infrared BH), 0.9 MHz (infrared CSP), and 0.6 MHz (visible CSP), respectively, is obtained from a least-square fit of the data points (cf. Table I).

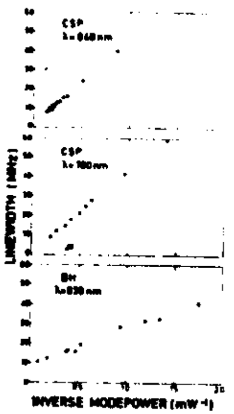

Fig. 1. Spectral linewidth versus inverse mode power per facet for an infrared CSP laser (upper part), a visible CSP laser (center part), and an infrared BH laser (lower part).

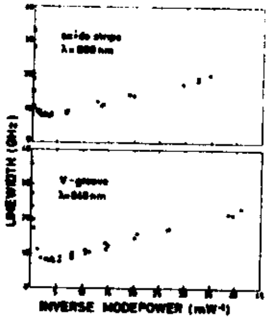

Fig. 2. Spectral linewidth versus inverse mode power per facet for an oxide stripe laser (upper part) and a V-groove laser (lower part).

Fig. 2 depicts the experimental results for the gain-guided lasers [oxide stripe (upper part) and V-groove (lower part)]. The linewidth is generally larger by roughly a factor of 1000, as compared to the index-guided lasers. Both laser types (V-groove and oxide stripe), again, behave in a similar fashion; a linear dependence of the linewidth $\Delta\nu$ on the inverse optical mode power P^{-1}_{mode} is found for relatively small mode powers (25-200 μW). A least-square fit to these data points results in an intercept of 6.5 GHz for both lasers and a slope of 385 MHz · mW for the V-groove and 376 MHz · mW for the oxide stripe laser, respectively (cf. Table I). At high mode powers (200 μW-11 mW) (CW and pulsed operation), however, the linewidth does not decrease with mode power, but instead, increases again. At the highest mode power of 11 mW (corresponding to a emitted total power of 150 mW), a linewidth of 43 GHz is obtained, which is even higher than the width at threshold.

DISCUSSION

The linewidth data will be analyzed according to [4], [5]

$$\Delta\nu = \Delta\nu_0 + \frac{h \cdot \nu \cdot v_g \cdot \alpha_m}{8\pi} \frac{R_{spon}}{P_{mode}} (1 + \alpha^2) \qquad (1)$$

where $\Delta\nu_0$ is a power-independent contribution to the linewidth, ν is the laser frequency, P_{mode} is the power per laser mode (per facet), v_g is the group velocity, α_m is the mirror loss ($\alpha_m = (-1/l) \ln R$, l is the cavity length, R is the mirror reflectivity), R_{spon} is the spontaneous emission rate per laser mode, and the enhancement factor α accounts for the index fluctuations, as will be discussed below. The spontaneous emission rate per laser mode is equal to the stimulated emission rate per laser photon multiplied by the astigmatism factor K, according to the Einstein relations, and thus,

$$R_{spon} = g n_{sp} v_g K \qquad (2)$$

and

$$n_{sp} = \{1 - \exp[-(\Delta E_F - h\nu)/kT]\}^{-1}$$

where n_{sp} accounts for incomplete population inversion, g is the optical gain, and ΔE_F is the separation of the quasi-Fermi levels.

Summarizing, the different contributions to the linewidth can be distinguished as follows [(1)].

a) Phase fluctuations of the optical field in the cavity introduced by spontaneously emitted photons at a rate R_{spon} leading to an inverse mode power dependence according to the Schawlow-Townes relation [1].

b) Index fluctuations caused by the coupling of phase and amplitude of the electric field and introduced by spontaneous emission. The ratio of the changes in real and imaginary parts of the dielectric function $\alpha = (\Delta n'/\Delta n'')$, finally, is a measure for the additional broadening arising from this mechanism [4].

c) A power-independent contribution $\Delta\nu_0$, which may account for different physical effects, e.g., refractive index fluctuations due to statistical fluctuations in the number of free electrons and holes. These fluctuations result in a contribution $\Delta\nu_0^1$ to the power-independent linewidth broadening, which can be described by [5]

$$\Delta\nu_0^1 = \frac{\Gamma \cdot \nu}{n} \cdot \delta N \cdot \frac{dn}{dN} \qquad (3)$$

where Γ is the confinement factor, ν is the laser frequency, n is the refractive index, δN is the carrier density fluctuation, and dn/dN is the change in refractive index with carrier concentration. Further contributions to $\Delta\nu_0$ will be discussed below.

First, the results for the index-guided lasers will be discussed. The power-independent contribution is almost the same for the visible (0.6 MHz) and infrared (0.9 MHz) CSP laser, and roughly a factor of ten higher for the BH laser (9.2 MHz). Welford and Mooradian [5] have calculated $\Delta\nu_0^1$ for a TJS laser to be about 2 MHz. Since for a CSP laser, the confinement factor has been estimated to be slightly smaller than for a TJS laser (0.2-0.4 for a CSP laser [10] instead of 0.4 for a TJS laser), the values obtained for the CSP lasers are quite reasonable. The fact that $\Delta\nu_0$ is smaller for the visible than for the infrared laser may be due to the lower threshold current (cf. Table I), thus, a smaller δN, which counterparts even for the frequency dependence of $\Delta\nu_0^1$. Even though the BH laser has a slightly higher confinement factor (0.6 [11]), it seems very unlikely that the value obtained for the BH laser can be explained on the basis of (3) alone. However, it should be noted that the spectral behavior for the BH laser is different from the CSP lasers. The BH laser shows a rather smooth transition between adjacent lasing modes as injection current is increased with regions where two lasing modes coexist. The CSP lasers, instead, show abrupt transitions between different lasing modes as the current is varied [12]. Therefore, we believe that the larger $\Delta\nu_0$ of the BH laser is related to the different mode behavior, as will be discussed in more detail for the gain-guided multimode lasers.

From the slope $\partial\Delta\nu/\partial P^{-1}_{mode}$ of the data of Fig. 1, the values for $R_{spon}(1 + \alpha^2)$ can be determined. The respective laser length, and hence the mirror losses α_m, are calculated from the measured mode spacing $\Delta\lambda$, assuming $v_g = c/4.33$ [10]. $R_{spon}(1 + \alpha^2)$, thus, amounts to $7.7 \times 10^{15}\ s^{-1}$, $19.7 \times 10^{15}\ s^{-1}$, and $10.3 \times 10^{15}\ s^{-1}$ for the infrared BH, the infrared CSP, and the visible CSP laser, respectively. If, for example, $\alpha = 5.4$ [4], [13] is assumed for all three lasers, R_{spon} is equal to $2.6 \times 10^{14}\ s^{-1}$, $6.6 \times 10^{14}\ s^{-1}$, and $3.4 \times 10^{14}\ s^{-1}$ for the respective lasers. If, on the other hand, R_{spon} is assumed to be constant (for example, $5 \times 10^{14}\ s^{-1}$), α has to be varied by a factor of 1.6 (α = 3.8, 6.2, and 4.4, again, for the three lasers). Unfortunately, no independent measurement of α or R_{spon} is available for the investigated lasers. The observed differences in slope, however, can be reasonably explained by respective variations of the parameters entering into (1). These differences may be attributed to either the spontaneous emission rate per laser mode R_{spon} or the enhancement factor α.

Next, the results of the gain-guided lasers will be discussed. We assume that the experimental results still can be described by (1). The important differences with respect to the laser linewidth of the gain-guided lasers as compared to the index-guided lasers are:

a) the emission spectrum of the gain-guided lasers, in general, consists of several longitudinal modes, and

b) the guiding is mainly accomplished by the imaginary part of the refractive index, resulting in an astigmatism of these lasers and in a modified spontaneous emission rate per laser mode [14], [15].

The slope $\partial\Delta\nu/\partial P^{-1}_{mode}$ in the case of gain-guided lasers is always larger than that for index-guided lasers. From the slope, we again obtain for the product $R_{spon}(1 + \alpha^2)$ values of $2.2 \times 10^{17}\ s^{-1}$ and $2.1 \times 10^{17}\ s^{-1}$ for V-groove and oxide stripe lasers, respectively. Assuming the same enhancement factor as for the index-guided lasers, e.g., $\alpha = 5.4$, $R_{spon} = 7.3 \times 10^{15}\ s^{-1}$, and $7.0 \times 10^{15}\ s^{-1}$ follows for the V-groove and oxide stripe lasers, respectively, which is roughly an order of magnitude higher than for the index-guided lasers. This difference in R_{spon}, indeed, is expected because the spontaneous emmission rate per laser mode is enhanced by the astigmatism of gain-guided lasers. The spontaneous emission rate per laser mode for typical gain-guided lasers has been calculated to be a factor of ten higher than for index-guided GaAs/(GaAl)As lasers [14], which well accounts for the characteristic difference in R_{spon} observed for index- and gain-guided lasers, though an additional difference in the enhancement factor α, due to the different guiding mechanism, might be possible.

The effect of the astigmatism on the laser linewidth is demonstrated even more drastically at the higher output powers (P_{mode} > 200 μW). The laser linewidth increases again in this regime (cf. Fig. 2), in contrast to the expected decrease as described by (1). The astigmatism factor K, which reflects the lateral electromagnetic field distribution in the cavity [15], [16] can be determined experimentally from the far-field distributions of the emitted laser light. We have measured the near- and far-field patterns simultaneously in order to check whether the astigmatism also changes at the higher output power. Fig. 3 shows some experimental results for the far-field pattern of the oxide stripe laser and its change with

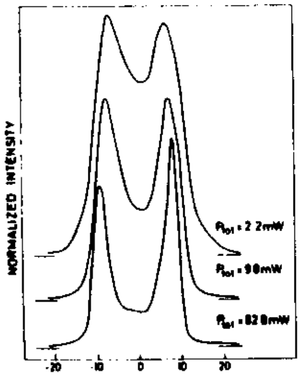

Fig. 3. Far-field patterns of an oxide stripe laser for three different optical output power levels.

output power. We find the peculiar far-field distribution with the so-called "ears," caused by the astigmatism [16], [17]. The change of the ratio of the maximum intensity corresponding to the ears $[I(\Theta_1)]$ to the intensity at the angle $\Theta = 0$ degree $[I(\Theta = 0)]$ directly reflects the change of the astigmatism factor K [18], i.e.,

$$K \propto I(\Theta_1)/I(\Theta = 0).$$

The relative change of K with output power as obtained from the far-field data (Fig. 3) is depicted in Fig. 4(c). We find an increase of the astigmatism factor by roughly a factor of 4 for the highest output level, as compared to low output power. This increase of the astigmatism factor is also reflected in the half width of the spectral envelope. The width of the envelope $\Delta\lambda_{spectrum}$ is directly proportional to the astigmatism factor and the inverse total power P_{tot} [19]. The product of $\Delta\lambda_{spectrum}$ and P_{tot}, therefore, is an additional measure for K. The experimental result is plotted in Fig. 4(b). We again find an increase of the astigmatism (about a factor of 6) in good agreement with the far-field data [cf. Fig. 4(c)]. The deviation of the measured linewidth from the expected value as obtained by extrapolating the linear part of the data of Fig. 2 [according to (1)] is finally plotted in Fig. 4(a). The ratio of the measured and extrapolated linewidth corresponds approximately to the change of the astigmatism factor as seen by comparing the results shown in Fig. 4. It thus seems very likely that the additional linewidth broadening at high output power is related to the change in astigmatism factor, and hence to the electromagnetic wave distribution in the resonator.

Finally, we discuss the power-independent contribution to the laser linewidth. $\Delta\nu_0$ in gain-guided lasers is about a factor of 100–1000 higher than in index-guided lasers (cf. Table I). In the case of index-guided lasers, $\Delta\nu_0$ can be at least partly attributed to statistical changes in carrier density, as has been discussed before. In gain-guided lasers, $\Delta\nu_0$ is too large to be explained by these statistical fluctuations alone. In gain-guided lasers, however, additional fluctuations may arise from the competition of the various longitudinal laser modes. This mode competition clearly shows up as an

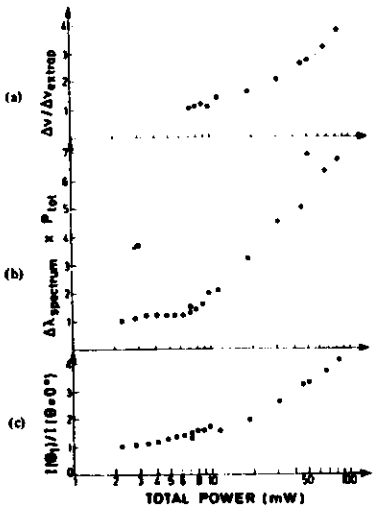

Fig. 4. Comparison of several spectral and waveguide properties of the gain-guided oxide stripe laser. (a) Ratio of the measured linewidth $\Delta\nu$ to the extrapolated linewidth $\Delta\nu_{extrap}$ as a function of the total optical output power per facet P_{tot} [obtained from Fig. 2(a)]. (b) Product of the half width of the spectral envelope $\Delta\lambda_{spec}$ and the total power P_{tot} versus total power P_{tot}. (c) Ratio of the maximum intensity of the far-field pattern $I(\Theta_1)$ to the intensity $I(\Theta = 0)$ at $\Theta = 0$ degree (obtained from Fig. 3) versus total output power P_{tot}.

additional contribution in the intensity noise of the individual laser mode [20], [21]. According to the classical rate equations for the phase and amplitude of the coupled laser modes [22], these intensity fluctuations result in phase fluctuations. These phase fluctuations, in turn, contribute to the laser linewidth and may account for the large power-independent contribution observed for gain-guided lasers. In addition, since this effect will be present in all multimode lasers, it should also contribute in index-guided lasers with a "nonideal single mode behavior," as observed for the BH laser discussed above. We therefore conclude that mode competition due to mode coupling in the dispersive medium of the active layer [23] introduces an additional line broadening in multimode lasers.

Summary

We have reported detailed investigations of the spectral width of single laser modes of gain- and index-guided GaAs/(GaAl)As semiconductor lasers. The linewidth of all the different index-guided lasers is typically on the order of 10–100 MHz and shows a linear variation with inverse mode power. The linewidth of a single longitudinal mode of a gain-guided laser is higher by three orders of magnitude and is typically in the range of a few GHz. Deviations from the expected dependence of laser linewidth on inverse mode power are additionally observed at high output power. The data of both laser types (gain- and index-guided) can be described by a modified Schawlow–Townes expression, taking into account the dependence of the spontaneous emission rate per

laser mode on the guiding mechanism, with additional broadening due to index fluctuations caused by spontaneous emission as well as a power-independent contribution. This power-independent contribution incorporates different physical processes, such as statistical carrier density fluctuations and phase fluctuations due to mode competition. No complete and self-consistent theory is available at present, however, to quantitatively account for these additional broadening mechanisms, which are unique to semiconductor lasers.

Acknowledgment

The authors wish to thank H. P. Vollmer (AEG-Telefunken), N. Chinone (Hitachi), and K. H. Zschauer (Siemens) for providing the laser diodes. The technical assistance of H. Klann and K. Rother is also gratefully acknowledged.

References

[1] A. Schawlow and C. H. Townes, "Infrared and optical masers," *Phys. Rev.*, vol. 112, pp. 1940–1949, 1958.
[2] D. E. McCumber, "Intensity fluctuations in the output of CW laser oscillators.I," *Phys. Rev.*, vol. 141, pp. 306–322, 1966.
[3] D. Welford and A. Mooradian, "Output power and temperature dependence of the linewidth of single-frequency CW (GaAl)As diode lasers," *Appl. Phys. Lett.*, vol. 40, pp. 865–867, 1982.
[4] C. H. Henry, "Theory of the linewidth of semiconductor lasers," *IEEE J. Quantum Electron.*, vol. QE-18, pp. 259–264, Feb. 1982.
[5] D. Welford and A. Mooradian, "Observation of linewidth broadening in (GaAl)As diode lasers due to electron number fluctuations," *Appl. Phys. Lett.*, vol. 40, pp. 560–562, 1982.
[6] A. Dandridge, "Measurements of the spectral characteristics of CW diode lasers," *Appl. Opt.*, vol. 20, pp. 2336–2337, 1981; also S. Saito and Y. Yamamoto, "Direct observation of lorentzian lineshape of semiconductor laser and linewidth reduction with external grating feedback," *Electron. Lett.*, vol. 17, pp. 325–327, 1981.
[7] M. W. Fleming and A. Mooradian, "Fundamental line broadening of single-mode (GaAl)As diode lasers," *Appl. Phys. Lett.*, vol. 38, pp. 511–513, 1982.
[8] A. R. Reisinger, C. D. David, K. L. Lawley, and A. Yariv, "Coherence of a room-temperature CW GaAs/GaAlAs injection laser," *IEEE J. Quantum Electron.*, vol. QE-15, pp. 1382–1387, Dec. 1979; also Ch. H. F. Velzel and R. P. Brouwer, "Output power and coherence length of stripe-geometry double-heterostructure semiconductor lasers in incoherent feedback," *IEEE J. Quantum Electron.*, vol. QE-15, pp. 782–786, Aug. 1979.
[9] D. D. Cook and F. R. Nash, "Gain-induced guiding and astigmatic output beam of GaAs lasers," *J. Appl. Phys.*, vol. 46, pp. 1660–1672, 1975.
[10] G.H.B. Thompson, *Physics of Semiconductor Laser Devices*, Chichester, England: Wiley, 1980.
[11] C. H. Henry, "Theory of the linewidth of semiconductor lasers," *IEEE J. Quantum Electron.*, vol. QE-18, [13], Feb. 1982.
[12] N. Chinone, K. Takahashi, T. Kajimura, and M. Ojima, "Low-frequency mode-hopping noise of index-guided semiconductor lasers," in *Proc. 8th IEEE Int. Semiconductor Laser Conf.*, Ottawa, Canada, 1982, Paper 25.
[13] It has been shown that the enhancement factor for different index-guided lasers is of the same order; C. Harder, K. Vahala, and A. Yariv, "Direct measurement of the linewidth enhancement factor α," in *Proc. 8th IEEE Int. Semiconductor Laser Conf.*, Ottawa, Canada, 1982, PDP 4.
[14] K. Petermann, "Calculated spontaneous emission factor for double-heterostructure injection lasers with gain-induced waveguiding," *IEEE J. Quantum Electron.*, vol. QE-15, pp. 566–570, July 1979, also J. P. Wittke, "Spontaneous-emission-rate alteration by dielectric and other waveguiding structures," *RCA Rev.*, vol. 36, pp. 655–666, 1975.
[15] W. Streifer, D. R. Scifres, and R. D. Burnham, "Spontaneous emission factor of narrow-stripe gain-guided diode lasers," *Electron. Lett.*, vol. 17, pp. 933–934, 1981.
[16] K. Petermann, "Some relations for the far-field distribution of semiconductor lasers with gain-guiding," *Opt. Quantum Electron.*, vol. 13, pp. 323–333, 1981.
[17] W. Streifer, R. D. Burnham, and D. R. Scifres, "An analytic study of (GaAl)As gain guided lasers at threshold," *IEEE J. Quantum Electron.*, vol. QE-18, pp. 856–864, May 1982, also W. Streifer, D. R. Scifres, and R. D. Burnham, "Analysis of gain-induced waveguiding in stripe geometry diode lasers," *IEEE J. Quantum Electron.*, vol. QE-14, pp. 418–427, June 1978; and W. Streifer, R. D. Burnham, and D. R. Scifres, "Symmetrical and asymmetrical waveguiding in very narrow conducting stripe lasers," *IEEE J. Quantum Electron.*, vol. QE-15, pp. 136–141, Mar. 1979, and J. B. Delaney and J. K. Butler, "The effect of device geometry on lateral mode content of stripe geometry lasers," *IEEE J. Quantum Electron.*, vol. QE-15, pp. 750–755, Aug. 1979.
[18] G. Arnold, K. Petermann, and E. Schlosser, "Spectral characteristics of gain-guided semiconductor lasers," *IEEE J. Quantum Electron.*, this issue, pp. 974–980.
[19] W. Streifer, D. R. Scifres, and R. D. Burnham, "Longitudinal mode spectra of diode lasers," *Appl. Phys. Lett.*, vol. 40, pp. 305–397, 1982.
[20] K. Petermann and E. Weidel, "Semiconductor laser noise in an interferometer system," *IEEE J. Quantum Electron.*, vol. QE-17, pp. 1251–1256, July 1981.
[21] A. Dandridge and A. B. Tveten, "Phase noise of single-mode diode lasers in interferometer systems," *Appl. Phys. Lett.*, vol. 39, pp. 530–532, 1981.
[22] M. Sargent III, M. O. Scully, and W. E. Lamb, Jr., *Laser Physics*. London: Addison-Wesley, 1974.
[23] T. L. Paoli and J. E. Ripper, "Coupled longitudinal mode pulsing in semiconductor lasers," *Phys. Rev. Lett.*, vol. 22, pp. 1085–1088, 1969.

Wolfgang Elsässer was born in Pforzheim, West Germany, on September 29, 1954. He received the Dipl. Phys. degree from the University of Karlsruhe, Karlsruhe, Germany in 1980.

In 1981, he joined the Max-Planck-Institut für Festkörperforschung, Stuttgart, where he is currently working towards his Ph.D. degree in the field of semiconductor lasers.

Mr. Elsässer is member of the German Physical Society.

Ernst O. Göbel was born in Seelbach, West Germany, on March 24, 1946. He received the Diploma degree in physics from the University of Frankfurt, Frankfurt am Main, West Germany, in 1970, and the Ph.D. degree in physics from the University of Stuttgart, Stuttgart, West Germany, in 1973.

In 1975 he was a Guest Scientist at Bell Laboratories, Holmdel, NJ, on a research fellowship of the Deutsche Forschungsgemeinschaft. From 1976 to 1980, he was with the University of Stuttgart working on semiconductor lasers and high excitation phenomena in semiconductors. In 1980 he joined the Max-Planck-Institut für Festkörperforschung, Stuttgart, where he is engaged in research on picosecond and femtosecond phenomena in solids, picosecond optoelectronics, and semiconductor lasers.

Dr. Göbel is member of the German Physical Society.

Jürgen Kuhl was born in Stendal, Germany, on January 23, 1940. He received the Diploma and Ph.D. degrees in physics from the Technische Universität Hannover, Hannover, West Germany, in 1966 and 1970, respectively.

From 1970 to 1975 he was a member of the Research Laboratories of Carl Zeiss, Oberkochen, Germany. He was involved in the development of flashlamp-pumped dye lasers and worked on nonlinear frequency mixing and trace analysis by fluorescence spectrometry. Since 1975 he has been Head of the Service Group for Optics and Spectroscopy at the Max-Planck-Institut für Festkörperforschung, Stuttgart, West Germany. His primary research interests are picosecond and femtosecond phenomena, nonlinear optics, and Fourier spectroscopy. He has been engaged in the development of several picosecond and femtosecond laser systems as well as their application for studying the ultrafast relaxation of "hot" carriers and phonons in solids.

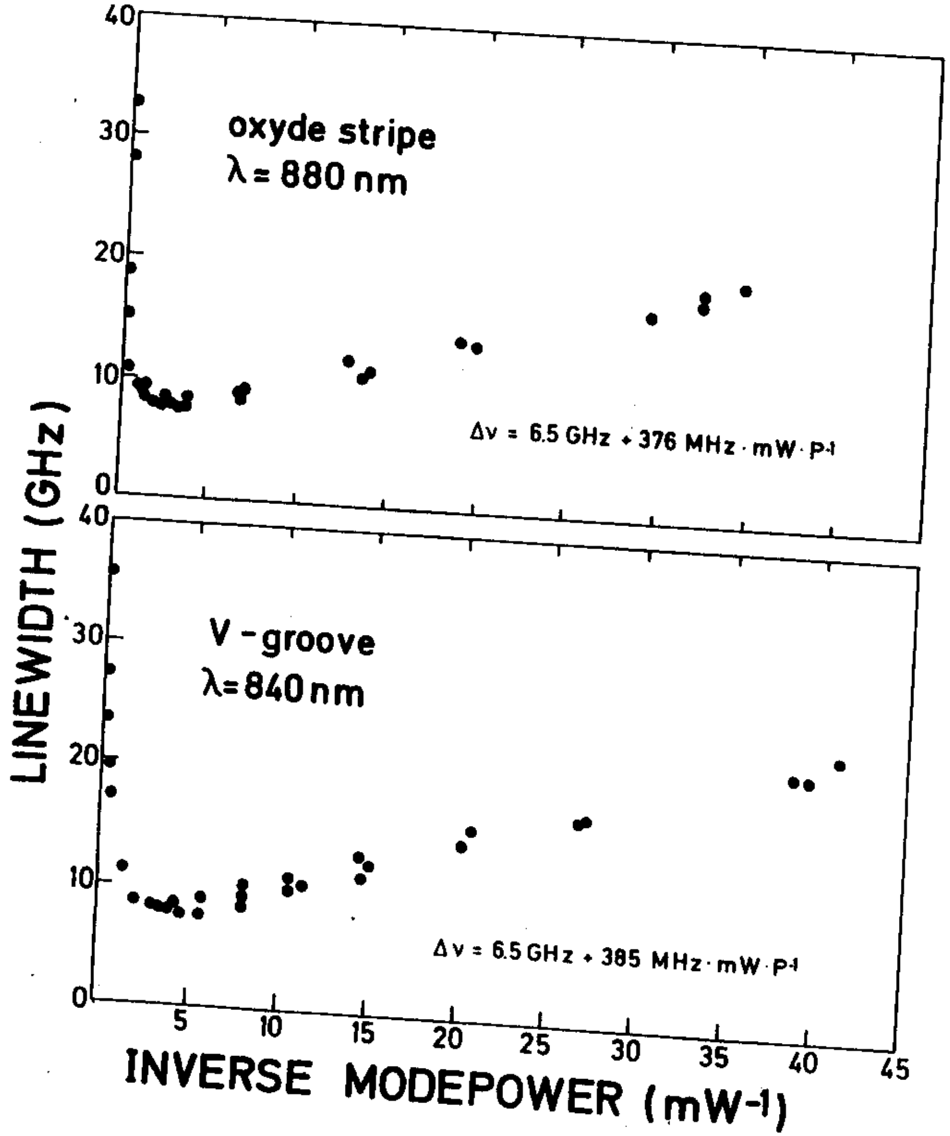

V. Elsässer & E. Göbel
IEEE J. Quant. Elect.

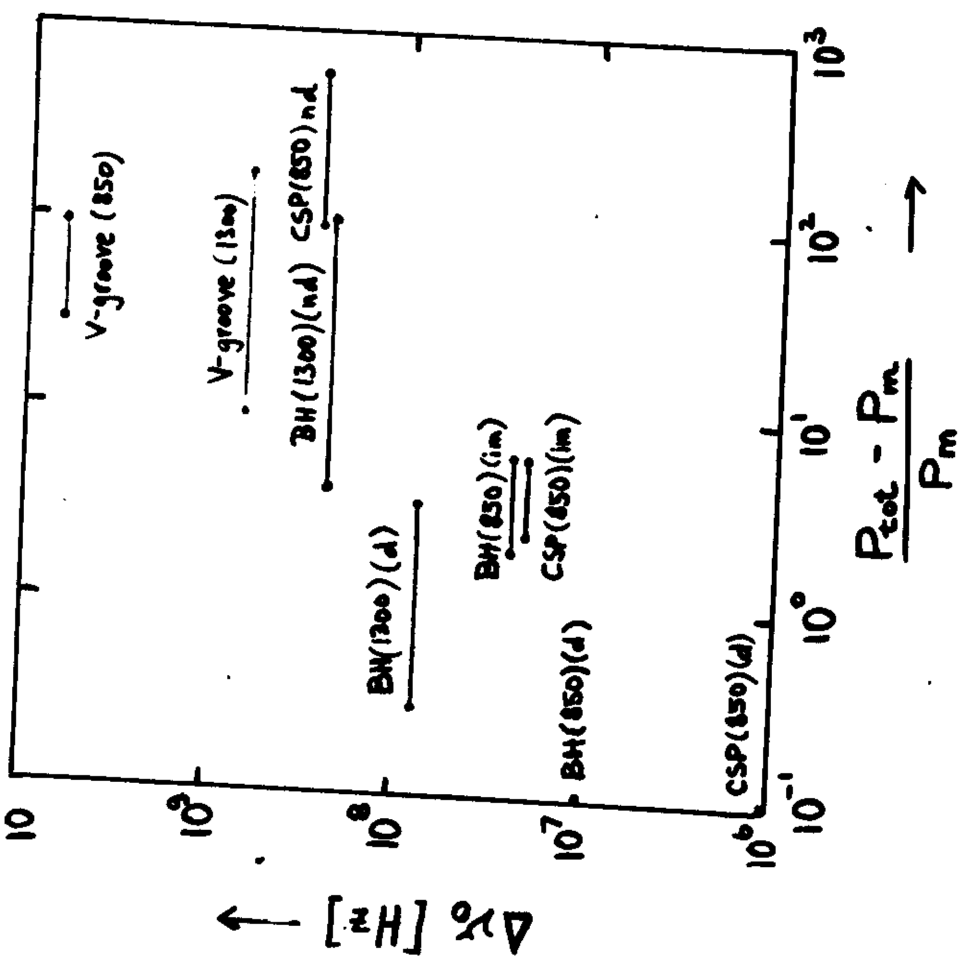

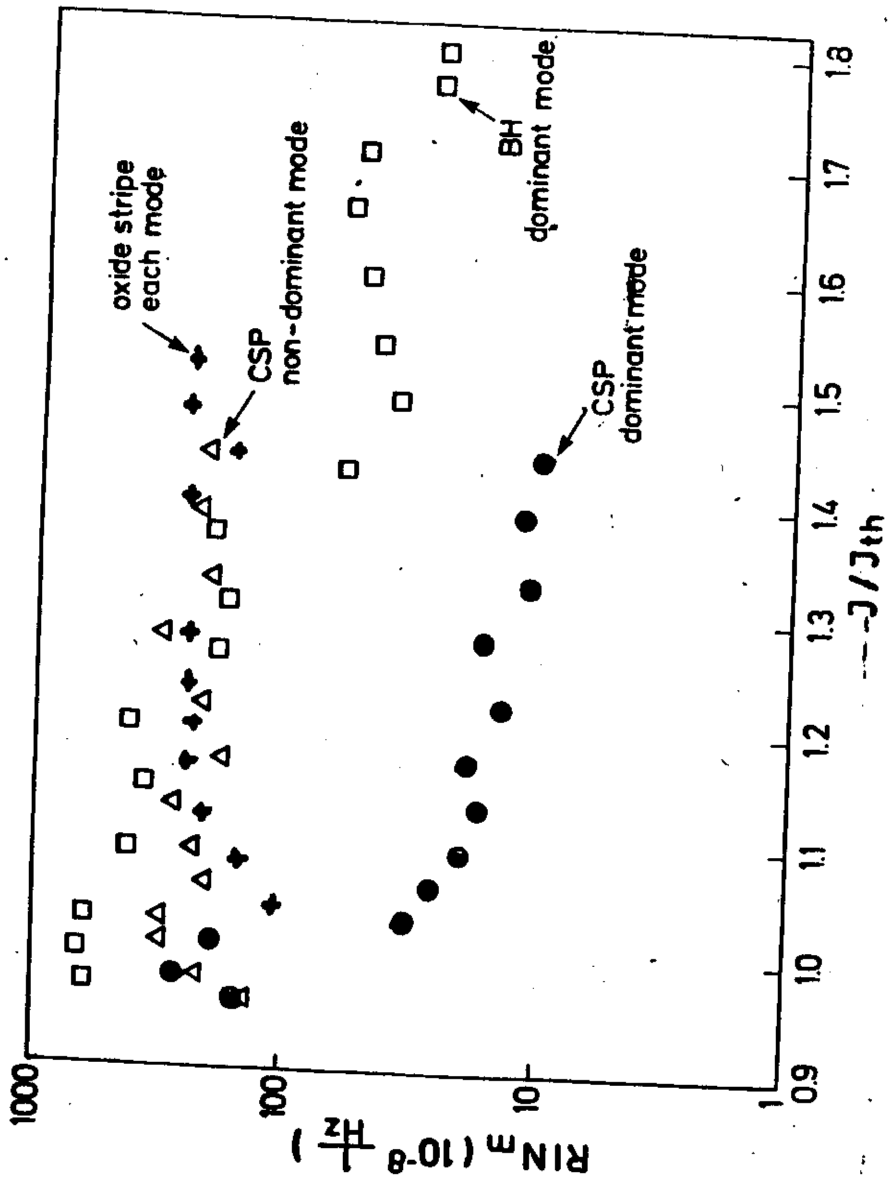

rate equations

$$\dot{E}_1 = E_1 (a_1 - \beta_1 E_1^2 - \theta_{12} E_2^2)$$

$$\dot{E}_2 = E_2 (a_2 - \beta_2 E_2^2 - \theta_{21} E_1^2)$$

$$\dot{\Phi}_1 = \Omega_1 - \nu_1 + \sigma_1 - \rho_1 E_1^2 - \tau_{12} E_2^2$$

$$\dot{\Phi}_2 = \Omega_2 - \nu_2 + \sigma_2 - \rho_2 E_2^2 - \tau_{21} E_1^2$$

- physical reason for $\Delta\nu$:

R_{spon}

self-emitted spontaneous photon

cross-emitted spontaneous photon

phase diffusion model

$\longrightarrow \langle \Phi^2 \rangle \longrightarrow \Delta\nu$

I. <u>weak coupling</u> $(\beta_1\beta_2 > \theta_{12}\theta_{21})$

$$\Delta\nu_1 = \frac{\langle \Delta E_j^2 \rangle \cdot R}{2\pi(\beta_1\beta_2 - \theta_{12}\theta_{21})^2}\left[\frac{(\rho_1\beta_2-\tau_{12}\theta_{21})^2}{E_{01}^2} + \frac{(\rho_1\theta_{12}-\tau_{12}\beta_1)^2}{E_{02}^2}\right] + \frac{\langle \Delta E_j^2 \rangle R}{2\pi\, E_{01}^2}$$

„$\Delta\nu_0$": $E_{01} \longrightarrow \infty$

$$\Delta\nu_1 = \frac{\langle \Delta E_j^2 \rangle R}{2\pi(\beta_1\beta_2 - \theta_{12}\theta_{21})^2}\,\frac{(\rho_1\theta_{12}-\tau_{12}\beta_1)^2}{E_{02}^2}$$

II. <u>neutral coupling</u> $(\beta_1\beta_2 = \theta_{12}\theta_{21})$

„$\Delta\nu_0$" : $E_{01} \longrightarrow \infty$

$$\Delta\nu_1 = \left[\sqrt[3]{\frac{\rho_1}{\beta_1}} + \sqrt[3]{\frac{\tau_{12}}{\theta_{12}}}\right]^2 \left(\sqrt[3]{\theta_{12}^2} + \sqrt[3]{\theta_{21}^2}\right) \sqrt[3]{\frac{2R\langle \Delta E_j^2 \rangle E_{02}^2}{\pi}}$$

PART III

PICOSECOND OPTOELECTRONICS

- Picosecond Optoelectronic Switches
- Modulation
- Mode Locking

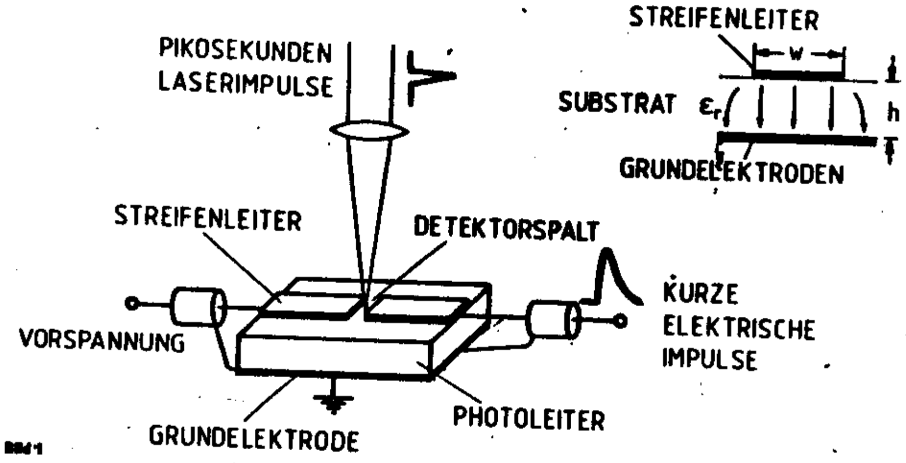

$$Z_L\,[\Omega] = 60 \cdot \ln(8\,h/w + w/4\,h)/\sqrt{\varepsilon_{eff}} \qquad \text{für } w/h \leq 1$$

$$Z_L\,[\Omega] = (120\pi/\sqrt{\varepsilon_{eff}}) \cdot (w/h + 1{,}39 + 0{,}67 \cdot \ln[w/h + 1{,}44]) \qquad \text{für } w/h \geq 1$$

wobei $\varepsilon_{eff} = 0{,}5 \cdot ([\varepsilon_r + 1] + [\varepsilon_r - 1]F)$

F = Geometriefaktor

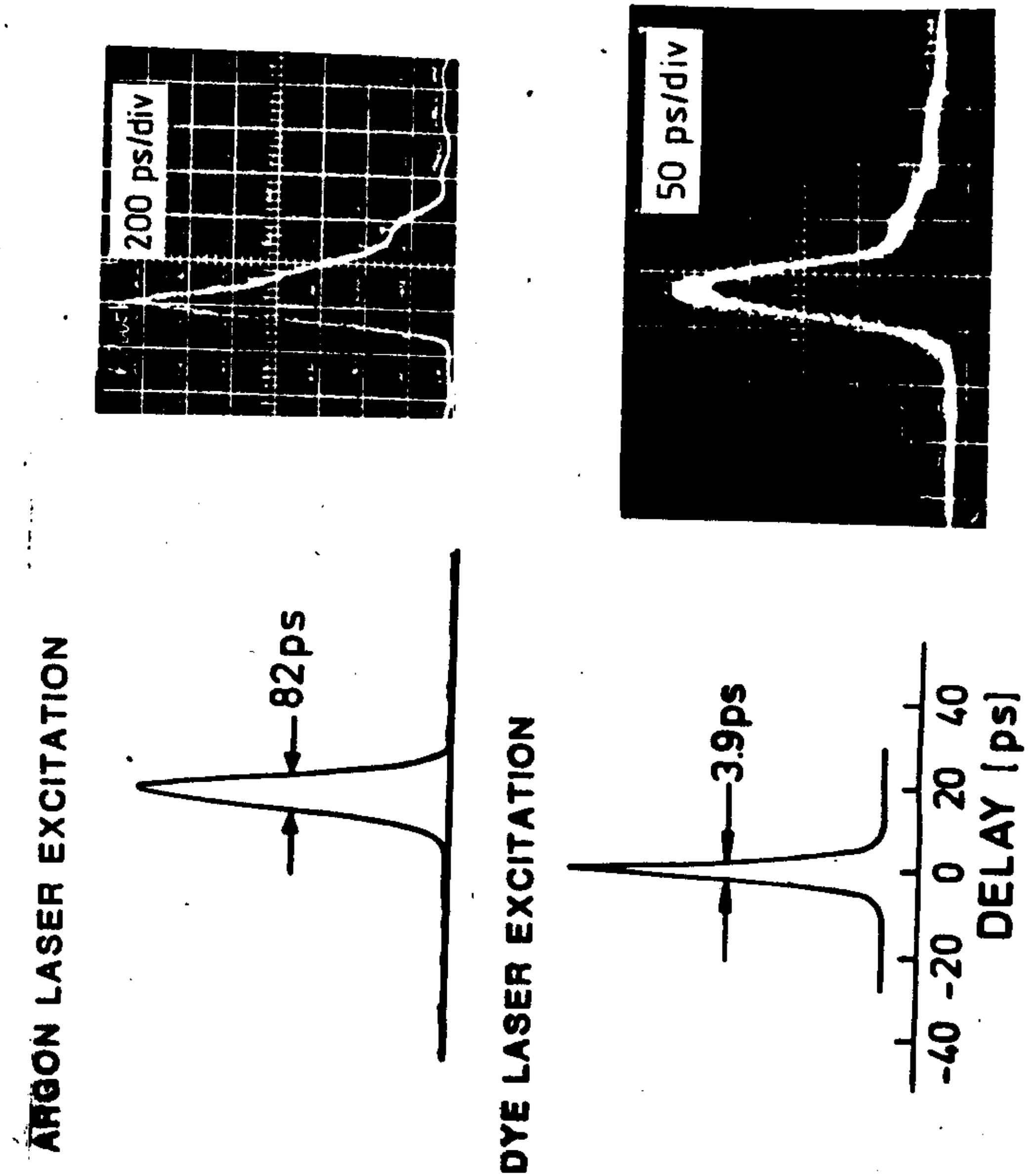

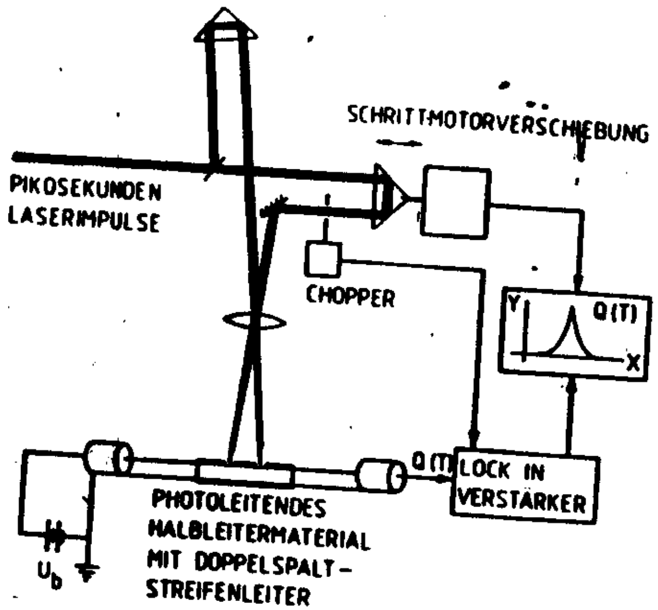

$$Q(T) \propto \int U(t) \cdot U(t+T)\, dt,$$

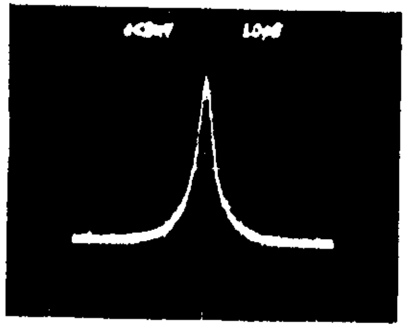

Pikosekunden elektrischer Impuls

erzeugt mit einem a-Si Schalter

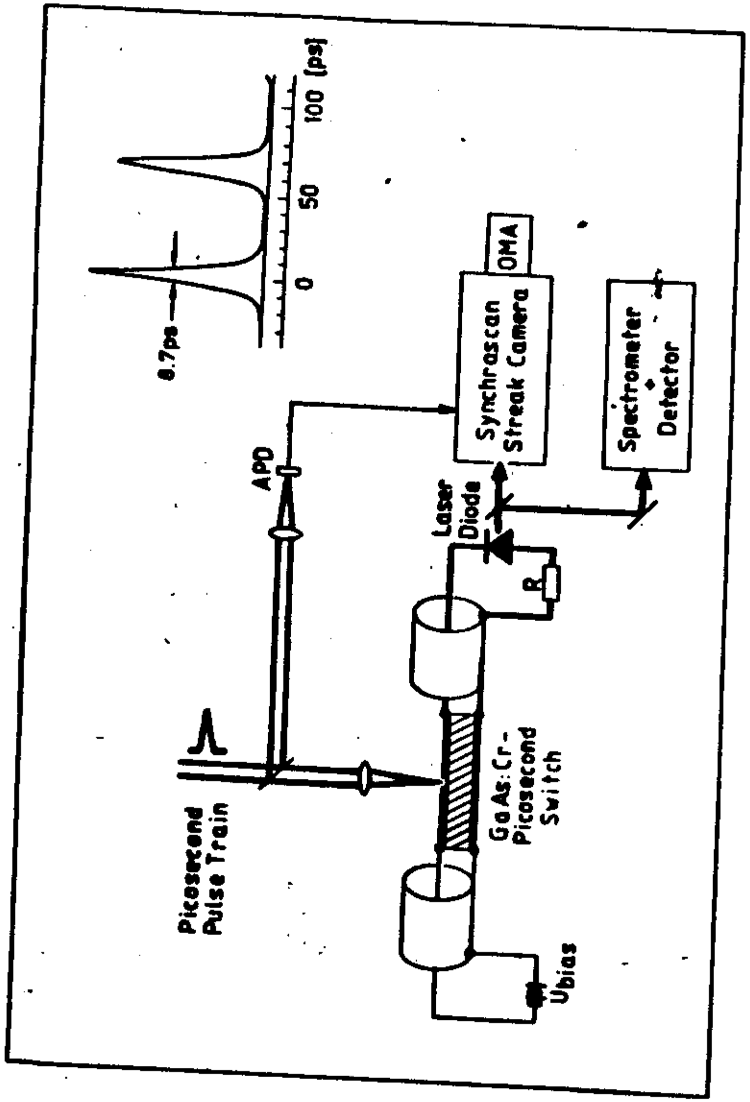
Picosecond Pulse Train
GaAs:Cr-Picosecond Switch
Ubias
APD
Laser Diode
R
Synchrascan Streak Camera
OMA
Spectrometer + Detector
8.7ps
0
50
100 [ps]

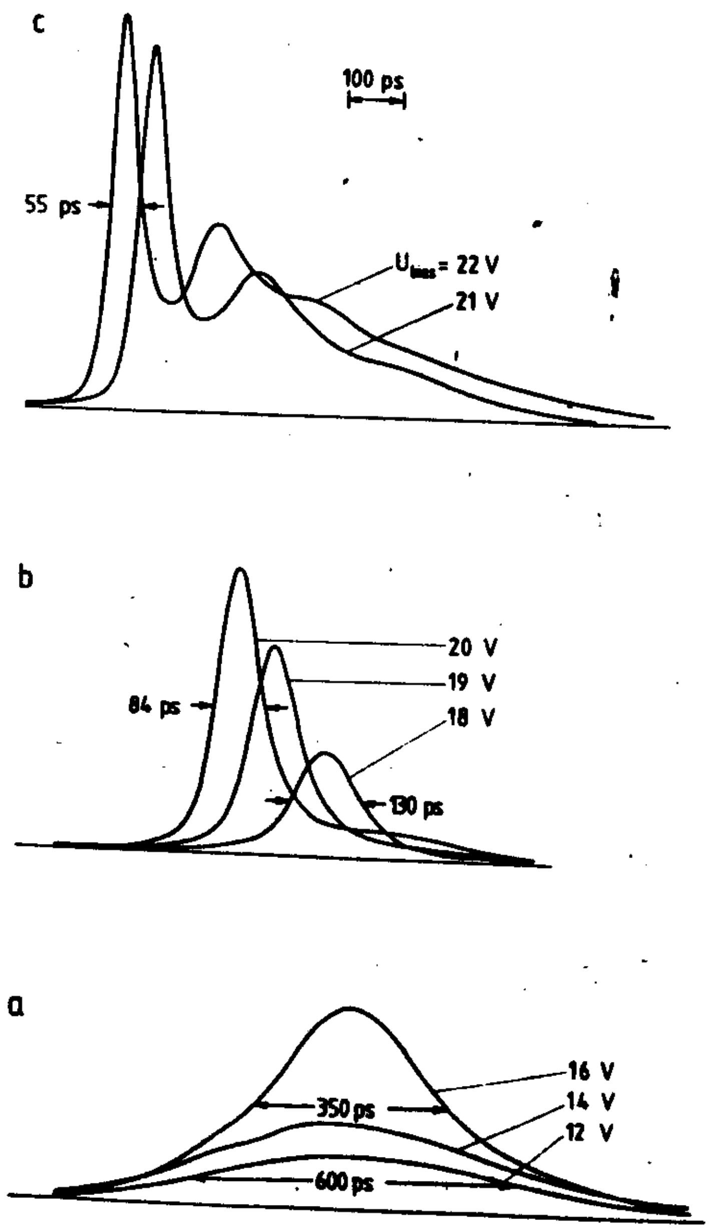
c
55 ps
100 ps
Ubias = 22 V
21 V
b
20 V
19 V
18 V
84 ps
130 ps
a
16 V
14 V
12 V
350 ps
600 ps

EXPERIMENT

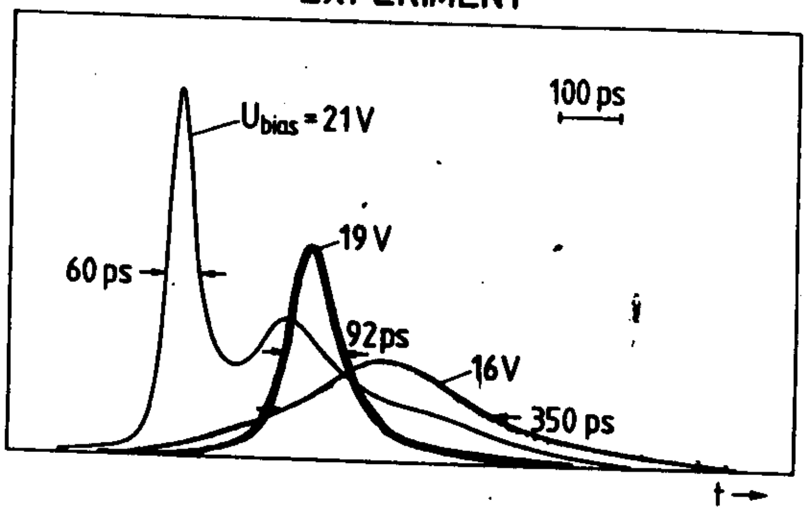

THEORY (RATE EQUATION MODEL)

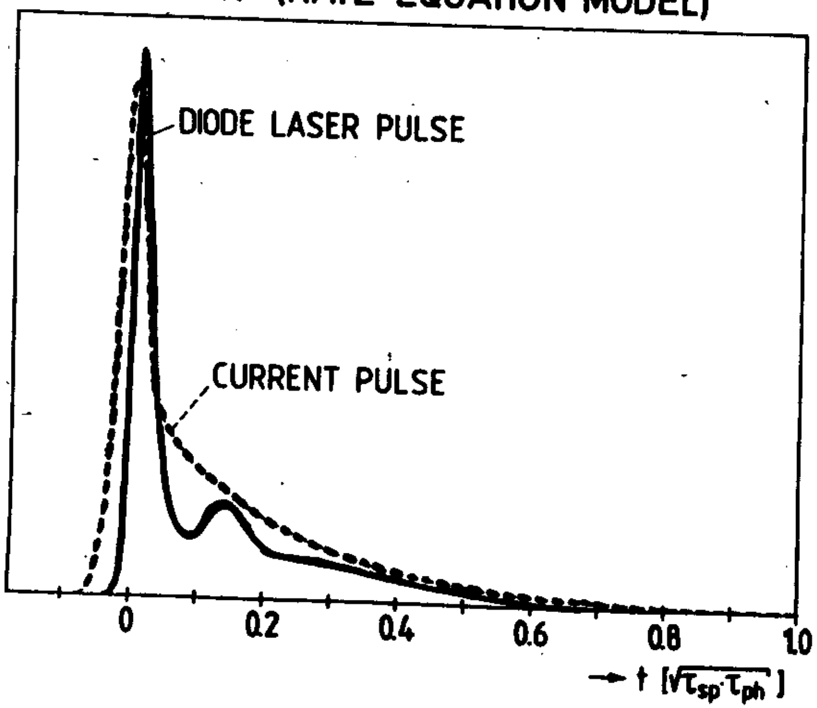

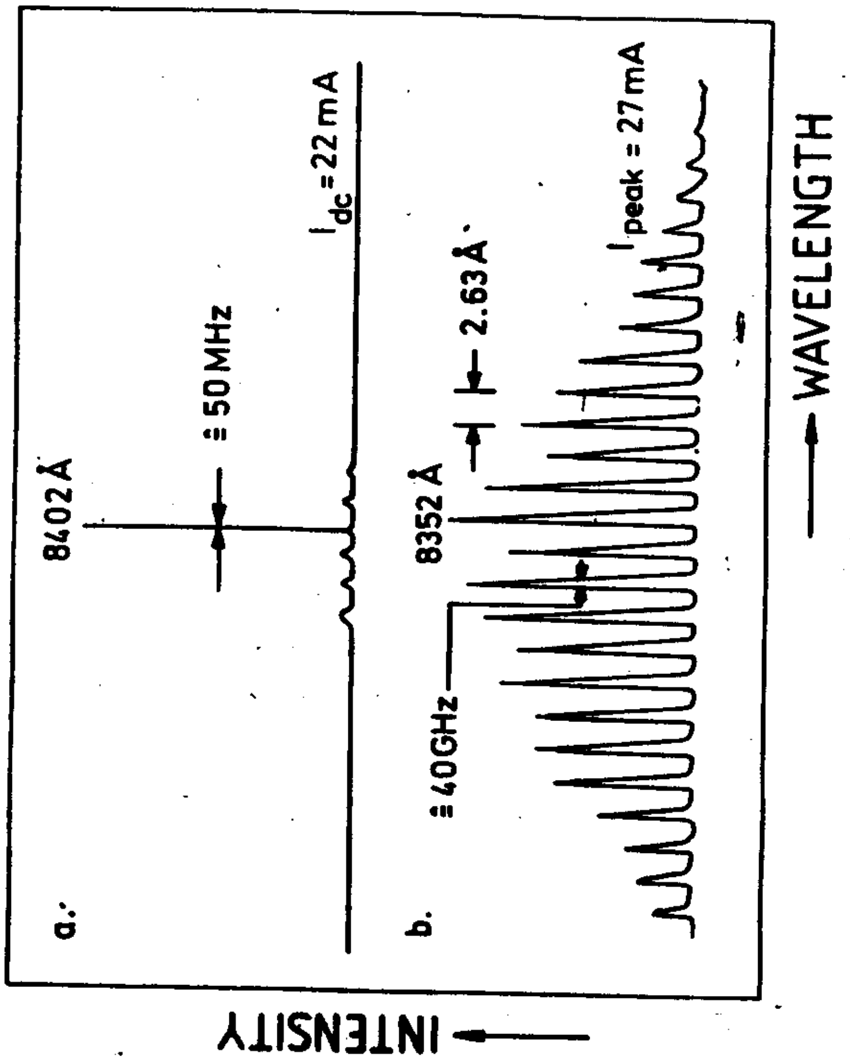

BH LASER (index guided) WITHOUT DC BIAS

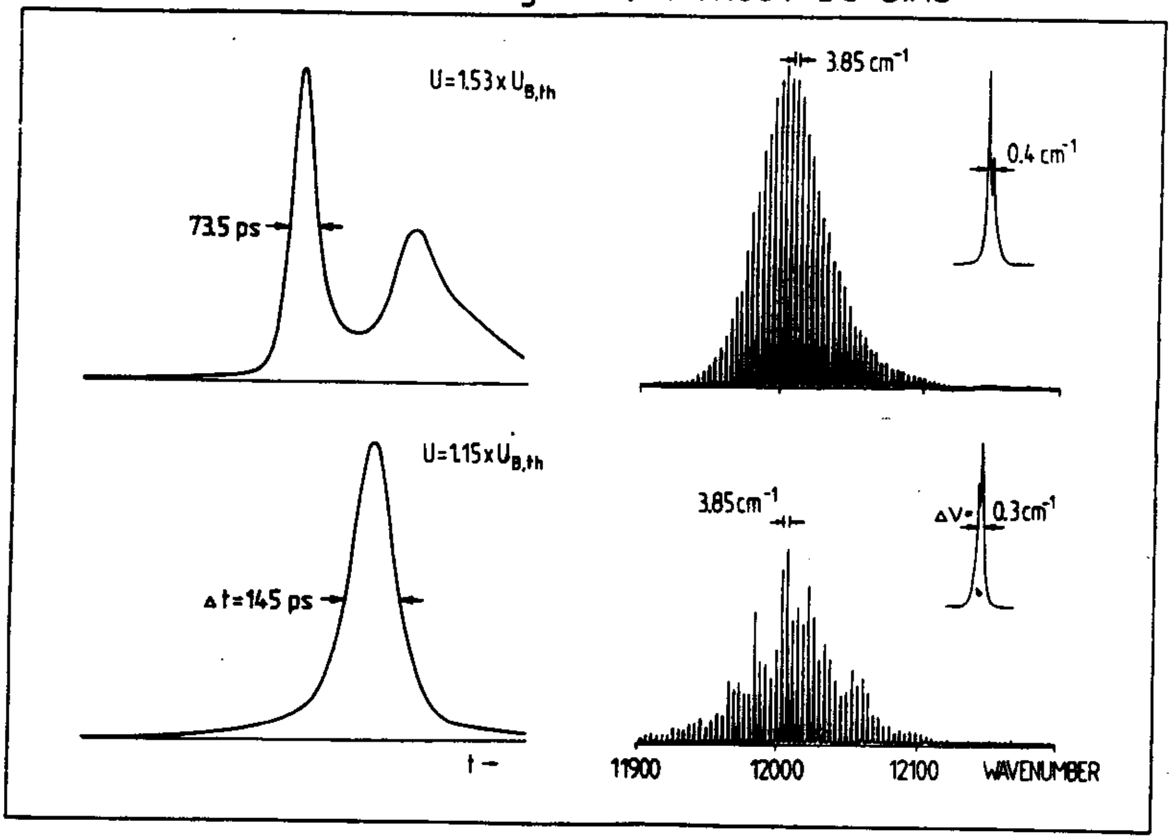

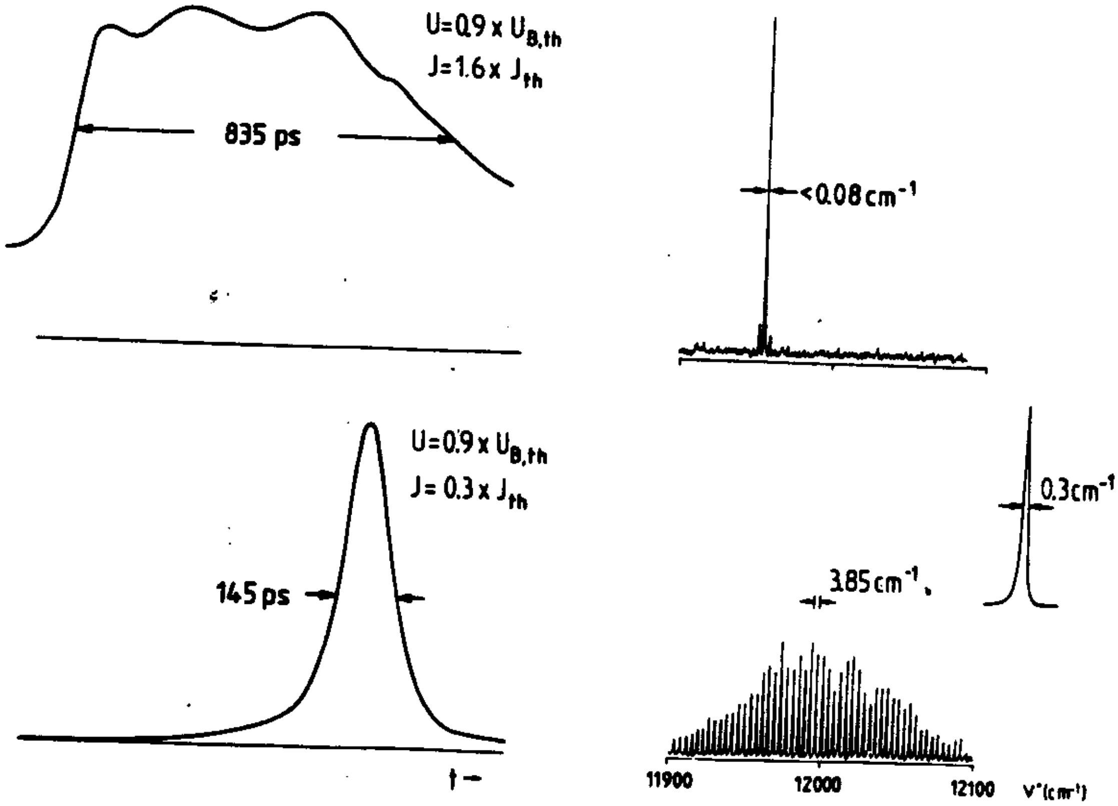

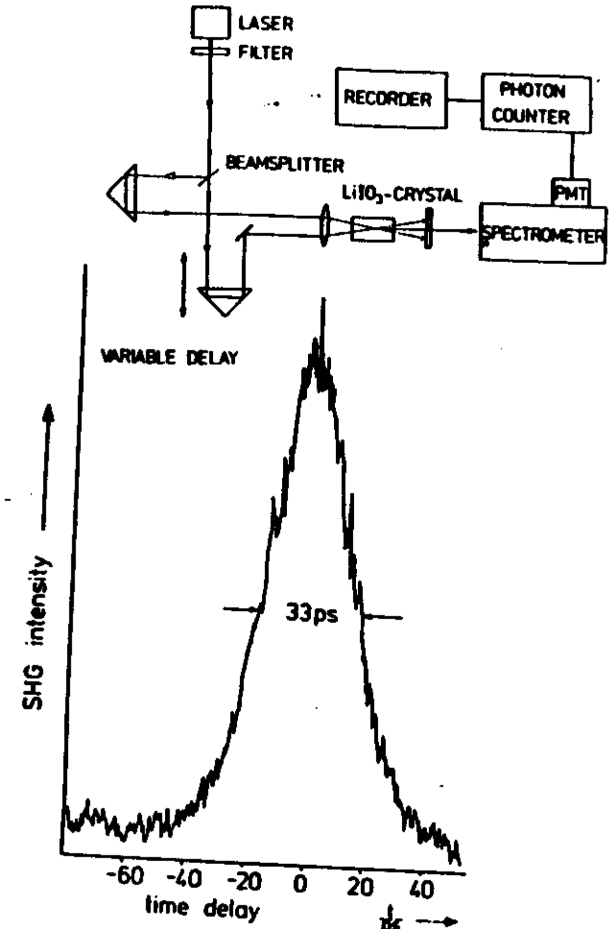

FIG. 3. SHG autocorrelation trace of the laser pulse. The half-width of the autocorrelation trace is 33 ps, corresponding to a 23-ps pulse width for a gaussian profile. The insert shows the block diagram of the setup for the autocorrelation experiments using SHG.

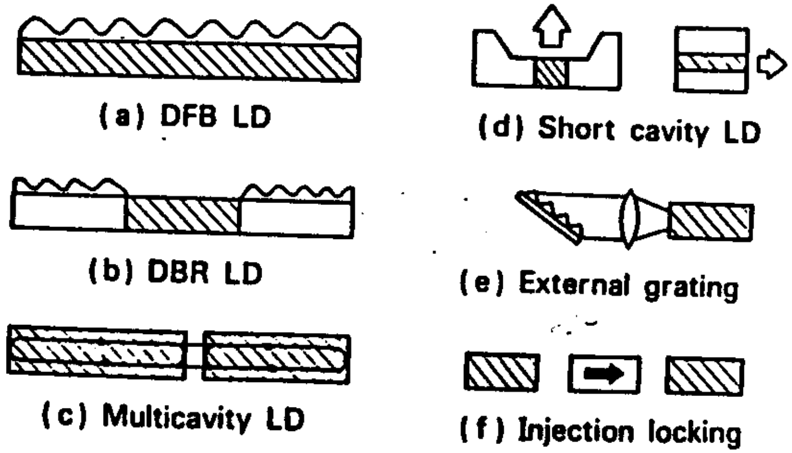

Fig. 1.1.1 Various axially mode controlled lasers.
(a) DFB,[34~46] (b) DBR,[47,48] (c) Multicavity,[23~27] (d) Short cavity[31~33] (e) External grating,[30] (f) Injection locking.[68~70]

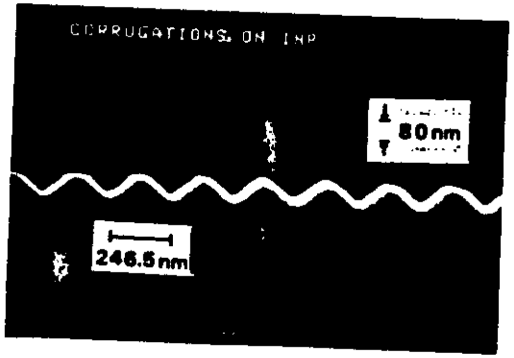

Fig. 1.1.17 SEM photograph of the first-order corrugation transcribed on InP substrate with the pitch and the depth of 246.5 nm and 80 nm, respectively.

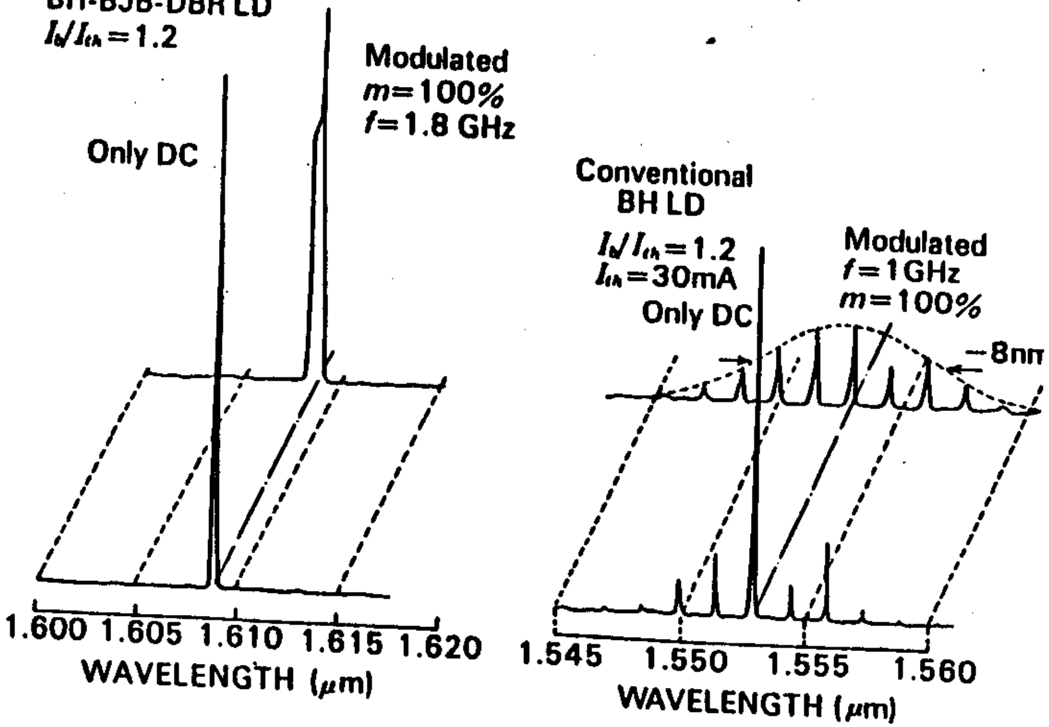

. 1.1.24 Time-averaged lasing spectrum under a rapid direct modulation of (a) a BH-DBR-BJB laser in comparison with that of (b) a conventional BH laser fabricated from the same wafer.[105]

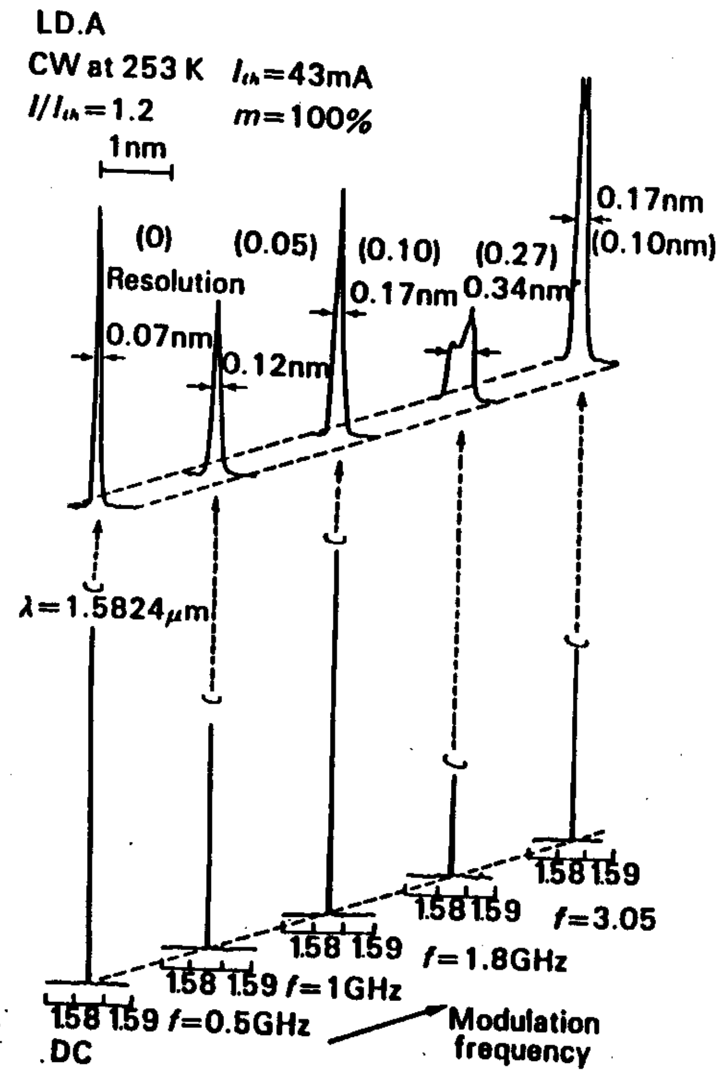

1.1.25 Time-averaged lasing spectra of a BH-DBR-ITG laser at various modulation frequencies. Magnified spectra are shown in the upper side, where the dynamic wavelength shift (nm) is indicated in the parentheses.[7)]

Mode-Locking

aktiv

passiv

aktiv-passiv

Synchronous pumping

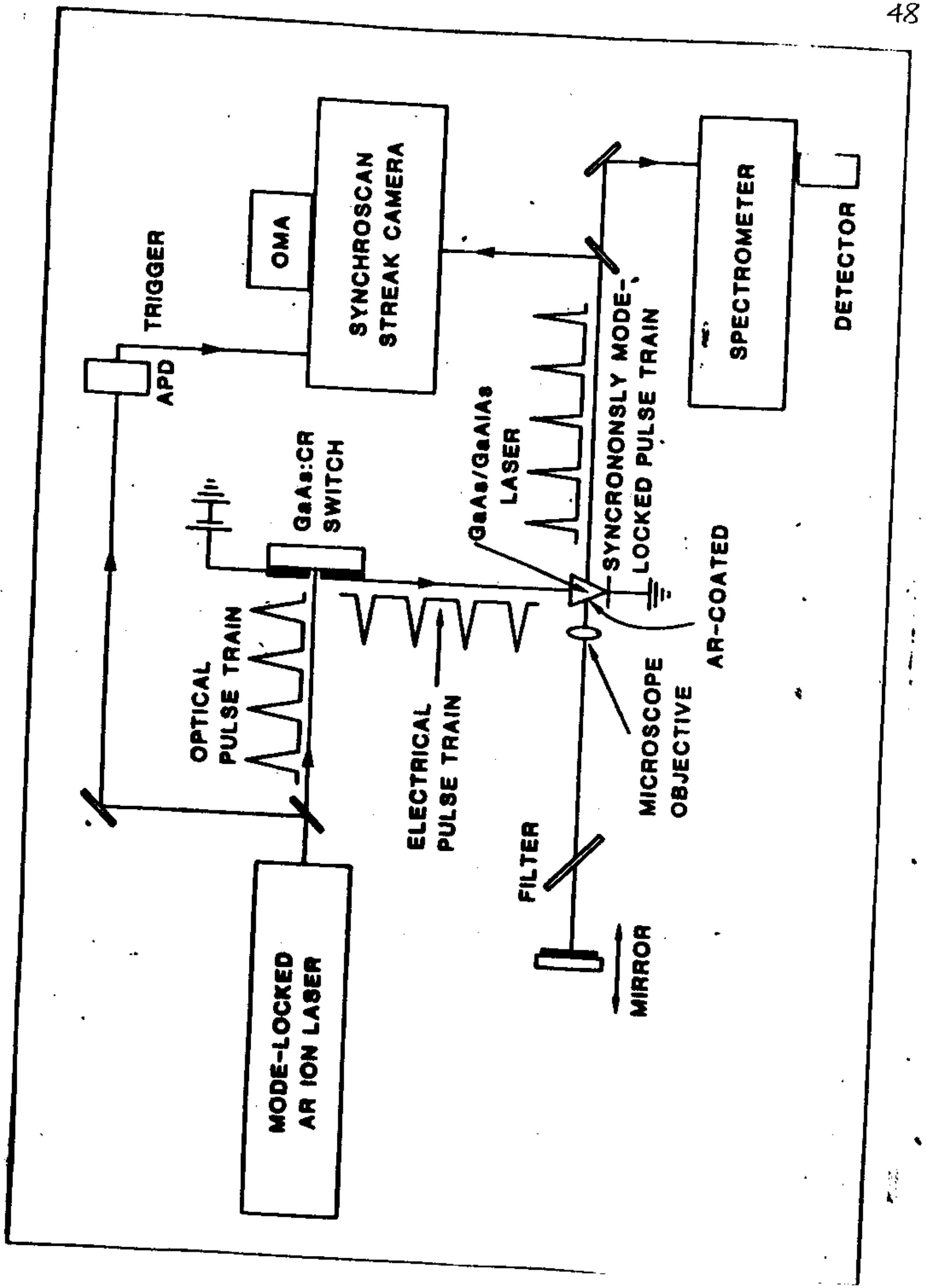
TRIGGER
APD
OMA
SYNCHROSCAN STREAK CAMERA
SPECTROMETER
DETECTOR
GaAs:CR SWITCH
GaAs/GaAlAs LASER
SYNCRONONSLY MODE-LOCKED PULSE TRAIN
AR-COATED
OPTICAL PULSE TRAIN
ELECTRICAL PULSE TRAIN
MICROSCOPE OBJECTIVE
FILTER
MIRROR
MODE-LOCKED AR ION LASER

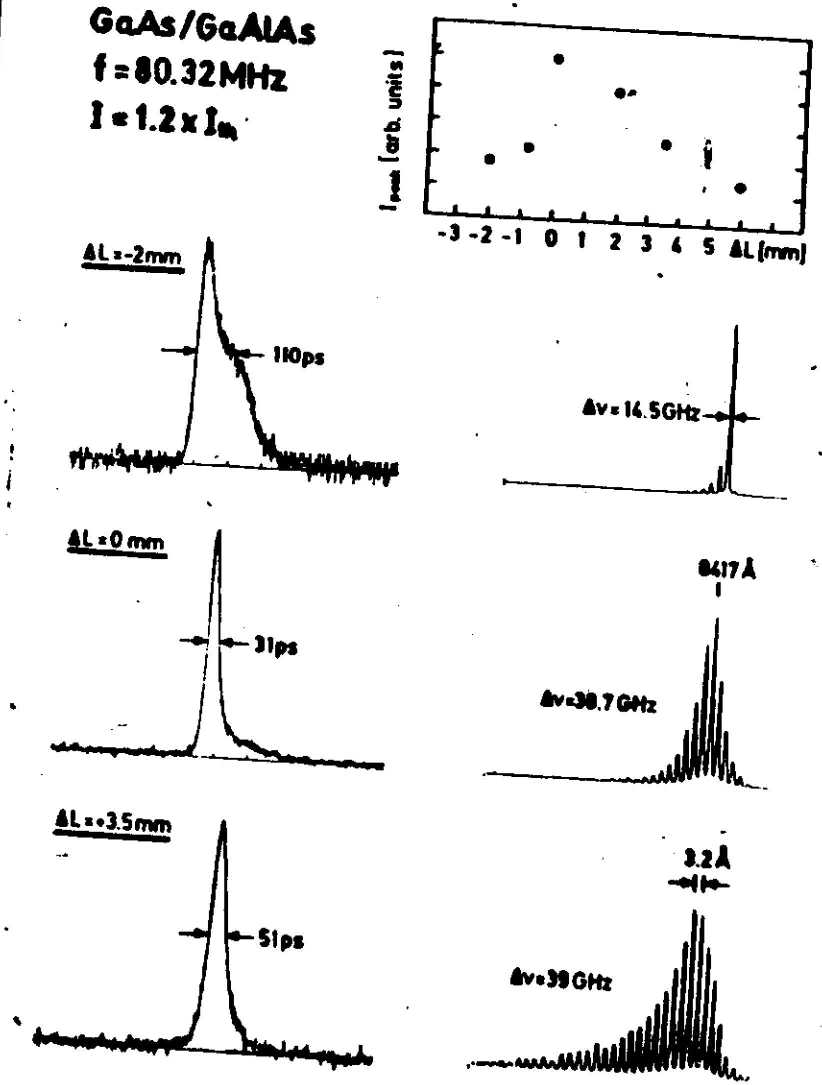
GaAs/GaAlAs
f=80.32MHz
I=1.2 x I_th
I_peak (arb. units)
-3 -2 -1 0 1 2 3 4 5 ΔL (mm)
ΔL=-2mm
110ps
Δν=14.5GHz
ΔL=0 mm
31ps
8417 Å
Δν=30.7 GHz
ΔL=+3.5mm
51ps
3.2 Å
Δν=39 GHz

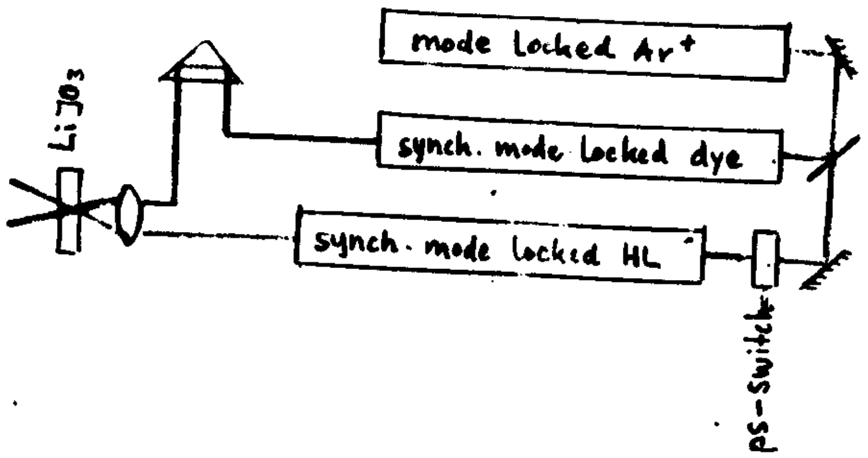

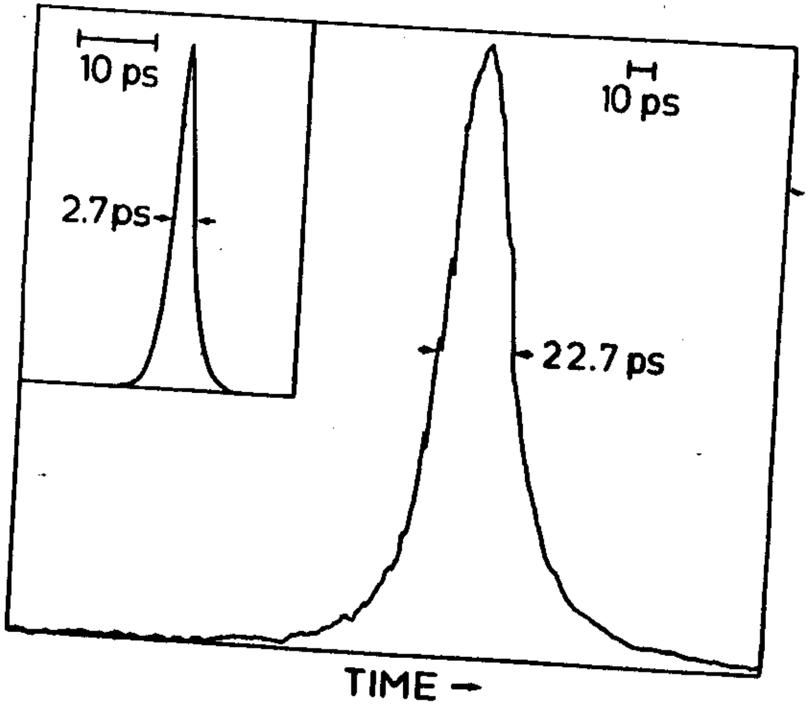

DIODE LASER PARAMETERS

PULSE DURATION Δt	:	30 ps
WAVELENGTH λ	:	8417 Å
BANDWIDTH Δν	:	1.3 cm^{-1}
Δν·Δt	:	1.2
AVERAGE POWER		250 μW
PEAK POWER		100 mW
PULSE ENERGY		2.5 pJ
		≙ 10^7 PHOTONS

FOURIER TRANSFORMATION (FT)

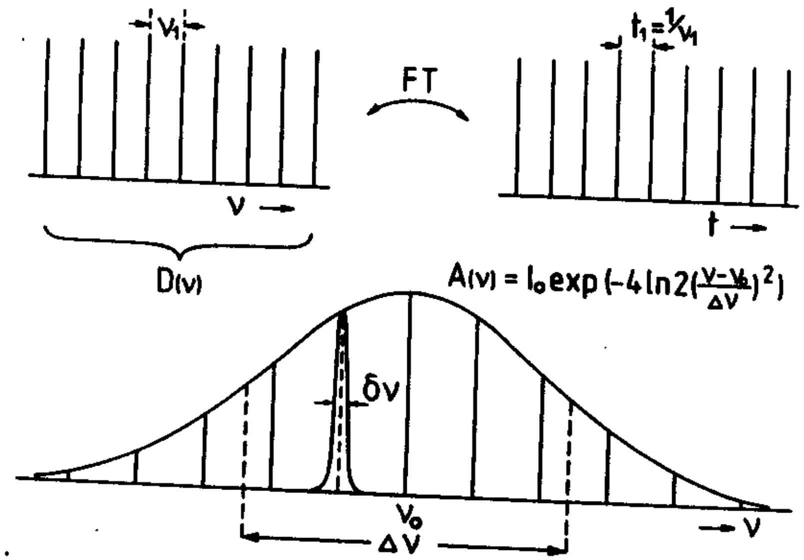

$B(\nu) = I'_0 \exp(-4\ln 2(\frac{\nu-\nu_0}{\delta\nu})^2)$

$$I(\nu) = A(\nu) \cdot (B(\nu) \otimes D(\nu))$$

$$I(t) = FT(I(\nu)) = B(t) \cdot (A(t) \otimes D(t))$$

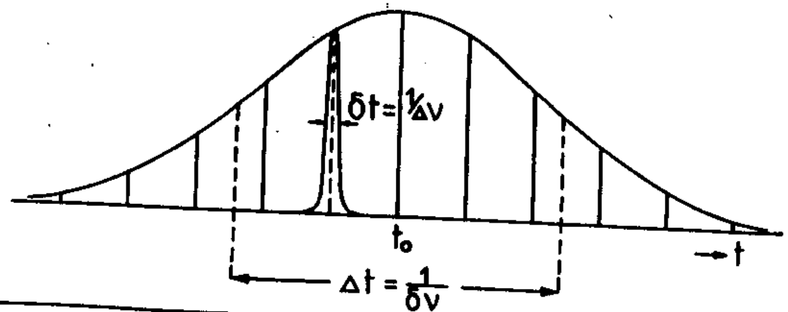

RED SHIFT DUE TO DECREASE OF CARRIER DENSITY DURING OPTICAL PULSE GENERATION

$$\frac{\delta\lambda_k}{\lambda_k} = 0.8\left(\frac{\delta n_k}{n_k} + \frac{\delta L}{L}\right).$$

BAND TO BAND TRANSITIONS IN GaAs

$$\delta n_k / n_k = -1.3 \times 10^{-21}\,\delta N$$

$$\delta N = -5 \times 10^{16}\,cm^{-3} \rightarrow \delta\lambda_k = 0.45\,Å$$

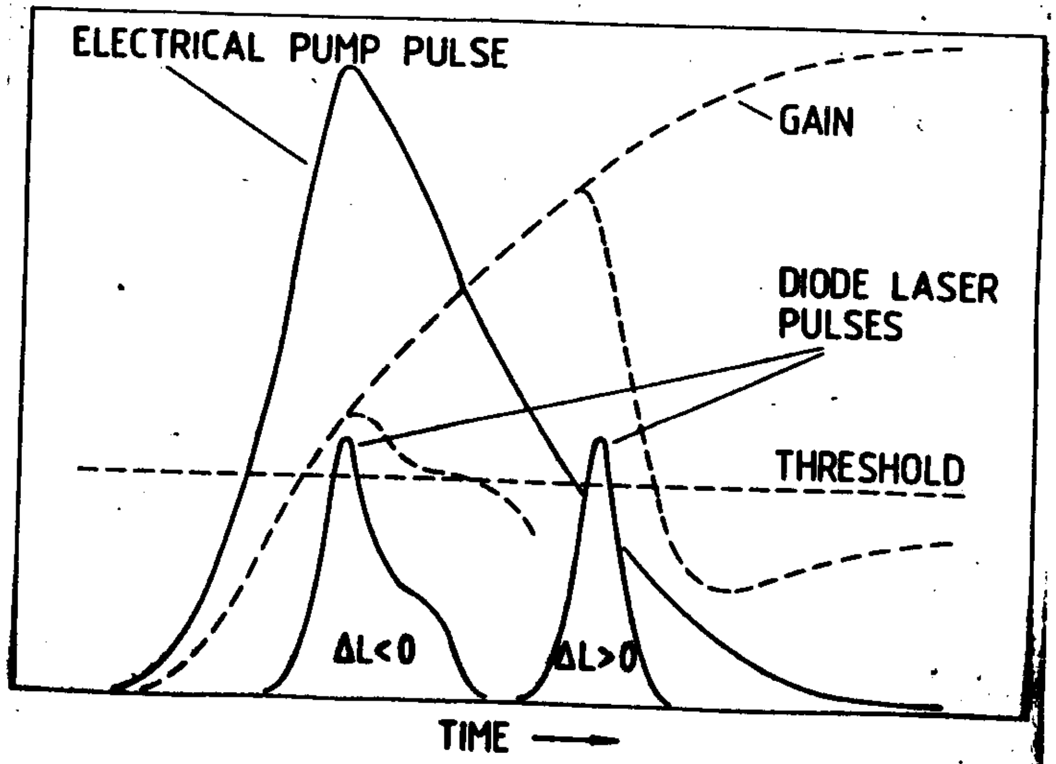

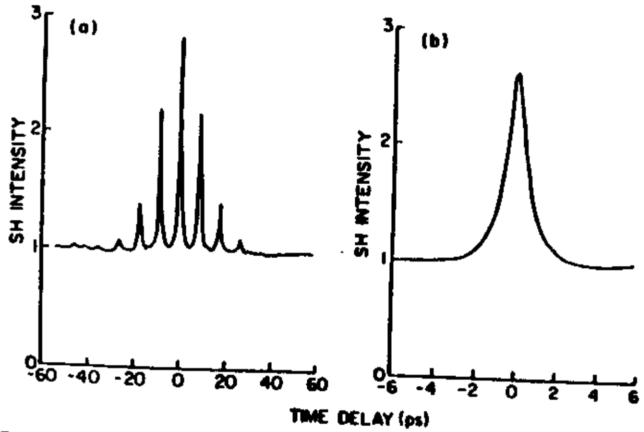

Fig. 13. Pulses generated by Yokoyama *et al.* (1982); $I = 1.50 I_{th}$, $L = 23$ mm. (a) Second harmonic of a pulse train which is formed by a single pulse bouncing several times in the diode, each time transmitting a portion of its energy through the cleaved face. (b) Magnification of the central part of (a). The width is 0.58 ps for a Lorentzian pulse shape.